

AWPM  
G84  
1983

SURFACE PROPERTIES OF BINARY MIXTURES OF BENZENE, TOLUENE,  
AND ETHYLBENZENE WITH DECANE AT THE AIR-LIQUID  
AND WATER-LIQUID INTERFACES

BY

MICHAEL J. GUMKOWSKI

A thesis submitted in partial fulfillment of  
the requirements for the degree of

MASTER OF SCIENCE

(Pharmacy)

at the

UNIVERSITY OF WISCONSIN-MADISON

1983

Pharmacy  
~~AXUM~~  
684

For Francine  
and  
my family, including those still  
living in our hearts.

## ACKNOWLEDGEMENTS

I would like to express my sincere appreciation to:

Professor P. Mukerjee for his guidance and patience, for the physical insight which he contributed to this work, and for teaching me that every hour is important;

The American Foundation for Pharmaceutical Education, and the CIBA-GEIGY Corp. for three years of financial support associated with the 1980-82 CIBA-GEIGY Pharmaceutics Scholarship;

The University of Wisconsin-Madison Graduate School for financial support;

The post-doctoral members of our research group who taught me how to function in a laboratory, with a special thanks to Dr. C. "R. C." Ramachandran, whose advice I didn't always heed;

The friends who have been a source of support and encouragement as this work and the education associated with it were in progress;

My parents, Walter and Jean, whose teaching, example, sacrifice, and unconditional love are responsible for whatever good work I may accomplish;

And, Francine, my best friend, whose unceasing faith helped 'move a mountain' 1000 miles.

## TABLE OF CONTENTS

	<u>Page</u>
I. INTRODUCTION . . . . .	1
A. General Background, Purpose, and Review of Previous Work . . . . .	1
B. Scope and Aim. . . . .	18
II. EXPERIMENTAL . . . . .	20
A. Materials. . . . .	20
B. Methods. . . . .	20
1. Purification . . . . .	20
2. Drop-volume method for surface tensions. . . . .	20
3. Wilhelmy plate method for interfacial tensions . . . . .	22
4. Density measurements . . . . .	25
III. RESULTS. . . . .	26
IV. DISCUSSION . . . . .	47
A. Surface Tension Studies. . . . .	47
B. Interfacial Tension Studies. . . . .	58
C. Excess Volumes of Mixing . . . . .	76
D. Interfacial Excess Quantities and Application to Micellar Solubilization . . . . .	77
V. CONCLUSIONS. . . . .	101
VI. REFERENCES . . . . .	103

SURFACE PROPERTIES OF BINARY MIXTURES OF BENZENE, TOLUENE,  
AND ETHYLBENZENE WITH DECANE AT THE AIR-LIQUID  
AND WATER-LIQUID INTERFACES

BY

MICHAEL J. GUMKOWSKI

(Under the supervision of Professor Pasupati Mukerjee.)

For a comparative assessment of surface chemical behavior of simple aromatic compounds, the air-liquid surface tensions and water-liquid interfacial tensions of binary mixtures of benzene, toluene, and ethylbenzene in decane have been measured. Such systems are likely to be of interest also as models for the interactions of small aromatic compounds with lipid assemblies.

Surface tensions were measured using the drop-volume method, interfacial tensions using the Wilhelmy plate method. The results were compared with the values calculated from several theories for surface tensions of mixtures. The Prigogine-Marechal parallel layer model for surface tension as amended by Gaines has been found to provide a good fit to the surface tension vs. composition curves using one adjustable non-ideality parameter,  $\beta$ , which was of reasonable magnitude. However, the interfacial tension data are not reproduced by the same

equation employing a single interaction parameter. Further analysis of these results reveals the importance of the specific interactions with water.

Derived values for the initial spreading coefficients demonstrate the non-ideality effects on the interactions between water and the binary mixtures studied. Excess volumes on mixing, calculated from density measurements, indicate the effect of alkyl substitution on the non-idealities of mixtures of aromatics and decane. The interfacial excess values,  $\Gamma$ , calculated using several conventions, showed a decreased relative adsorption of the aromatic component with increasing chain length of the alkyl substituent. The results are used to describe the distribution of aromatic solubilizates between the core and the interface of micelles. It is found that the fraction of the solubilizate at the interface is significant and that this fraction decreases substantially as the total amount in the micelle increases. Such effects can influence the solubilization capacity, lipid-water distribution coefficients, and transport of small slightly polar molecules in lipid assemblies and similar systems having a high surface-to-volume ratio. Also, the stability of solubilized compounds whose reactivity is dependent upon exposure to hydrophilic species (e.g.,  $H^+$ ) will be affected. The results are found to be in qualitative agreement with

spectroscopic and viscometric studies of these compounds solubilized in micelles.

APPROVED:

Pasupati Mukerjee  
Professor Pasupati Mukerjee

DATE:

May 19, 1983

## I. INTRODUCTION

### A. General Background, Purpose, and Review of Previous Work

Lipids in solution may assemble in a variety of forms.<sup>1</sup> When the medium is aqueous, the primary driving force for the formation of these assemblies is the hydrophobic interaction.<sup>2</sup> Micelles, vesicles, liposomes, membranes, and lipoproteins are some examples of such assemblies. Industry and research have found or postulated many uses for these systems. Biologically, lipid membranes are integral to a variety of cellular functions. Mixed micelles containing bile salts play a central role in the solubilization and absorption of exogenous fats.<sup>3</sup> In practical pharmaceutical systems, liposomes have already been used for drug delivery<sup>4</sup> and micellar solutions are also widely employed as vehicles for many drugs.<sup>5</sup> Micelles and vesicles have been used to simulate complex biological enzymes and membranes.<sup>1</sup> An extensive literature has developed on the use of lipid assemblies, particularly micelles, to catalyze reactions or stabilize organic compounds in solution.<sup>6</sup> In the presence of lipid assemblies, the solubilities of many organic compounds are greater than in pure water.<sup>5,7-10</sup> This solubilizing power is due to the presence of lipid assemblies rather than the lipids themselves. In surfactant solutions very little solubilization

occurs below the critical micellization concentration (cmc).<sup>7</sup> The presence of micelles is a requirement for solubilization. Thus, monomeric lipids have little solubilizing power.

Clearly, then, with respect to both physiological function and technological applications one of the most important characteristics of lipid assemblies is their interaction with small organic molecules. A lipid assembly is composed of amphipathic molecules having both distinctly polar and predominantly hydrocarbon moieties or regions. The solubilizing properties of a lipid assembly are determined largely by the structure of the molecules which compose it. For example, a greater mole fraction of benzene is solubilized by cetyl trimethylammonium bromide (CTAB) micelles than sodium dodecyl sulfate (SDS) micelles.<sup>11,12</sup> Of course, the solubilization capacity of micelles depends also upon the nature of the solubilizate. In this respect micelles do not behave like a bulk hydrocarbon solvent. In fact, many highly polar molecules may be solubilized by micelles to a greater extent than are hydrocarbons. For example, at saturation the mole ratio of methyl isobutyl ketone to cetyl pyridinium chloride (CPC) in a 0.1M CPC solution is 2.02, while that of hexane is 0.49, and benzene 2.03.<sup>7,8</sup> Indeed, for all lipid assemblies one of the most important relevant factors is their uptake capacity for solubilizates, and the related partition behavior between

the aqueous medium and the lipid assembly.<sup>7</sup>

Many small molecules solubilized by lipid assemblies are known to interact with molecular or ionic species which have very low or negligible affinity for nonpolar environments.<sup>6</sup> Such species may be, for example, an hydronium ion or an enzyme. For such interactions to be possible, some solubilized molecules must reside close to the interface between the polar and non-polar regions of the lipid assembly in order to be accessible to polar reactants.<sup>7</sup>

The above facts and implications all serve to emphasize the special nature of the interactions of numerous physiological species, xenobiotics, and drugs with the vast network of such lipid assemblies in the body. Certainly, the nature of the interactions of drug molecules with biological membranes will affect many major events controlling a drug's fate in the organism, including transport, distribution, and metabolism. An understanding of the factors controlling the uptake, location, distribution, and orientation of small molecules in lipid assemblies is, then, of interest to pharmacy and technology. However, although the understanding of physiological lipid systems is one of several long-term objectives of research in this area, it should be stressed that such systems themselves are complex.<sup>13</sup> Indeed, the role of various lipid constituents, such as, cholesterol, in the structure and function of biological lipid assemblies may involve many of the

complicating factors already mentioned. In order to investigate the primary structural feature of an organic core and a polar exterior common to all lipid assemblies, simple model systems are required.

Micelles have been used as models for other lipid assemblies, because of their stability and simplicity of formulation. Classically, the micelle is viewed as a droplet of aliphatic hydrocarbon with a polar coat.<sup>13</sup> If solubilizates are themselves structurally complex, and, in particular, are themselves somewhat amphipathic, the interactions with lipid assemblies will involve orientational and other factors which may be of dominant importance. One of the major objectives of this research is the investigation of the role of the micelle-water interface in solubilization behavior. For a close-examination of this, simple aromatic molecules such as benzene, may be considered to be good model solubilizate species because aromatic-aliphatic systems have not been found to be highly non-ideal.<sup>14</sup> Indeed, such systems have been studied by a variety of experimental approaches for various purposes.

An early investigation by Riegelman, et al.<sup>15</sup> compared the ultraviolet spectra of many solubilized species to their spectra in isotropic solvents. The results indicated that the region of solubilization depended upon the chemical nature of the solubilizate. Eriksson and Gillberg<sup>16</sup> studied the effect of the solubilizate concentration on the proton

magnetic resonance line shifts of all identifiable protons of CTAB. The results suggested that benzene, nitrobenzene, and N,N-dimethylaniline were solubilized at the surface. At higher concentrations the line shifts were interpreted as indicating a transition toward solubilization in the core. Similar reasoning on the results for cyclohexane and isopropylbenzene suggested that these compounds were solubilized in the core at all concentrations. Rehfeld<sup>11</sup> used differential absorption spectroscopy to study the region of solubilization of benzene in SDS and CTAB micelles. He concluded that benzene resided primarily in the micellar core, although the environment of benzene within the micelle was expected to be non-uniform. Fendler and Patterson<sup>17</sup> studied the reactivity of hydrated electrons with solubilized benzene. In SDS the rate was decreased compared to water indicative of solubilization in the core. Reaction rate enhancement was noted when benzene was solubilized in CTAB micelles. Fendler, Day, and Fendler<sup>18</sup> examined the rate of change of the chemical shift as a function of concentration of benzene in micelles. The results suggested a surface location in SDS micelles but a core location in CTAB micelles. Fox et al.<sup>19</sup> used the line broadening of nmr spectra caused by paramagnetic ions to estimate the distance of p-xylene from the micellar surface. They concluded that p-xylene ranges freely throughout the hydrocarbon region of the SDS micelle.

Mukerjee and Cardinal<sup>20,21</sup> examined the effects of various solvents of graded polarity on some solvent sensitive spectral parameters derived from uv absorption bands of benzene and alkyl substituted benzenes. Such parameters determined for the aromatic species solubilized in aqueous micellar systems were compared with reference solvent data. Effective polarity estimates of the average microenvironment of the solubilized species could be obtained in this manner. For benzene in SDS and CTAB micelles, the average microenvironment was found to be somewhat closer to water than to hydrocarbon. Using a graded polarity scale of zero for hydrocarbons and unity for water, a semiquantitative estimate of the average polarity of the benzene environment was 0.65. In the case of the alkyl benzenes, the estimated average polarity of the microenvironments decreased with increasing alkyl substitution.

Recently, Simon et al.<sup>22</sup> have noted that the free energy of transfer of benzene to hydrocarbon and to micelles or lipid bilayers is quite similar. They have concluded that benzene resides primarily in a non-polar environment. Jobe et al.<sup>23</sup> have reported their study of ultrasonic spectroscopy in micellar sodium octyl sulfate solution. By measuring relaxation frequencies and amplitudes, they could assess the average locus of solubilization of a compound in the micelle. Cyclohexane was found to reside mostly in the micellar core. Benzene and toluene in

minute amounts could be found at the surface, but at higher concentrations were located principally in the core.

In an attempt to explain many of the above results, Mukerjee and Cardinal<sup>21</sup> have suggested a two-state model for micellar solubilization. Solubilized molecules are considered to be distributed between an "adsorbed" state at the interface between the polar and non-polar regions of the micelle and a "dissolved" state in the predominantly hydrocarbon core. At all concentrations an equilibrium must exist between these states. The tendency of a solubilize to favor the adsorbed over the dissolved state should be related to its ability to reduce the interfacial free energy of the micelle. Taking into account the high surface to volume ratio of a micelle, even the mild surface activity of aromatic species could result in a high fraction of solubilize at the surface.

Attempting to get a quantitative estimate of the fraction of benzene at a micellar surface, Mukerjee and Cardinal measured the dependence on benzene concentration of the interfacial tension at the oil-water interface of two-phase systems containing heptane, benzene, and water. From the slope of the resulting curve, the interfacial excess of benzene could be calculated. Extrapolation to micellar systems of the values obtained by this method was given some justification by an analysis<sup>21</sup> of some data presented earlier by Rehfeld.<sup>24</sup> He had measured the interfacial

tension of many hydrocarbon-water systems in the presence of varying amounts of SDS. The interfacial tension for benzene paralleled in a rough manner that of the alkane systems as SDS concentration was increased. The difference between the alkane-water and benzene-water tensions remained nearly the same over the range 88.8-66.4 Å<sup>2</sup>/molecule of SDS. This range includes the head group area per monomer determined for SDS micelles (71.4 Å<sup>2</sup>/molecule). This behavior would serve to indicate that the presence of SDS did not greatly affect the difference in the interfacial tensions between the two types of systems. It suggests that benzene dissolved in hydrocarbons would exhibit similar surface activity in the presence and absence of surfactants. Therefore, systems without surfactant could be used to estimate the surface activity and surface excess of benzene in a micelle to a certain degree of approximation which remains to be determined. This was also roughly consistent with the constancy of the estimated microenvironmental polarity of benzene, determined spectroscopically, when the head group of the micelle was changed from that of SDS to CTAB.<sup>21</sup>

Using the surface excess values obtained from the interfacial tension data, Mukerjee and Cardinal<sup>21</sup> showed that as the concentration of benzene was increased the mole fraction of benzene in the micellar core also increased. They used this result to explain the concentration

dependence of the microenvironmental polarity of benzene that had been noted by Eriksson.<sup>16</sup> This was also offered as an explanation for the differences in the conclusions of Fendler<sup>17</sup> and Rehfeld<sup>12</sup> who had studied the microenvironment of benzene in micelles at low and high concentrations, respectively.

Increasing the size of the alkyl substituent leads to an increase in the interfacial tension of alkylbenzenes against water.<sup>21</sup> Therefore, alkyl substitution reduces the driving force for adsorption. The tendency for alkylbenzenes to reside in a more hydrophobic average microenvironment could, therefore, be qualitatively explained by the two-state model.

This argument is also consistent with the concentration dependence of the viscosity of the surfactant solutions containing aromatic components. Smith and Alexander<sup>25</sup> have demonstrated that methyl cyclohexane does not increase the viscosity of CPC micellar solutions. Eriksson and Gillberg<sup>16</sup> have noted only slight increases in viscosity upon addition of cyclohexane or isopropylbenzene to CTAB solutions. However, benzene, toluene, and polar aromatic compounds produced a large increase in viscosity upon increasing the mole ratio of solubilizate to surfactant. At high concentrations of these solubilizates a decline in viscosity was noted. Mukerjee and Manabe<sup>26</sup> have studied the concentration dependence of the viscosity of

alkylbenzenes of increasing chain length in aqueous 0.1M CPC solutions. Toluene showed a sharp peak while ethylbenzene exhibited a much lower maximum occurring at a lower concentration. Propylbenzene and butylbenzene showed no maxima and only a small change in viscosity.

The formation of rodlike micelles, which can cause a viscosity increase of a micellar solution, is opposed by the interaction of the charged head groups of ionic surfactants.<sup>27</sup> Additives in the micelle which are adsorbed at the micellar interface will tend to reduce this repulsion.<sup>16,28</sup> As more solubilizate is added, the two-state model would suggest that a higher fraction of it will be dissolved in the core. However, as yet, no definitive explanation for the viscosity maximum has been offered.

The two-state model appears to provide a useful approach to describing the interactions occurring between micelles and solubilized species. Solubilization capacity, accessibility to attack by species located in the continuous phase, and interfacial orientations leading to site specific reactivity can all be addressed through this model. Many questions remain, however, concerning the fraction,  $f$ , of solubilizate in the adsorbed state, the effect on  $f$  caused by the type of lipid assembly employed, the effect of the interfacial microenvironment on  $f$ , and the prevalence of preferred interfacial orientations. In the case of small systems being discussed here, even a proper definition of  $f$

may involve rather detailed modelistic approaches for the interface. In this study we examine the possibility of estimating  $f$  from model bulk experiments on liquid-liquid interfaces. Determining the fraction adsorbed from bulk experiments requires a knowledge of the derivative of interfacial tension with respect to activity of one component. The assessment of the surface excess,  $\Gamma$ , by this method may not be feasible in many cases. Therefore, the usefulness of existing theories of surface and interfacial tensions of binary mixtures for predicting  $\Gamma$  should also be examined.

Both empirical<sup>29,30</sup> and theoretical<sup>31-40</sup> relationships have been developed to describe the concentration dependence of surface tension. In the simplest theoretical model, the assumption of a monolayer surface phase and a perfect solution, obeying Raoult's law at all concentrations gives:

$$\begin{aligned} \mu_i^b &= \mu_i^{0,b}(T,p) + RT \ln x_i^b = \mu_i^{0,s}(T,p) + \\ &RT \ln x_i^s - \gamma a_i = \mu_i^s \end{aligned} \quad (1)$$

where,  $\mu_i$  = the chemical potential of species  $i$ ,

$\mu_i^0$  = the chemical potential of pure component  $i$ ,

$x_i$  = the mole fraction of component  $i$ ,

$\gamma$  = the surface tension,

$a_i$  = the partial molar area of species  $i$ ,

$R$  = the molar gas constant,

$T$  = absolute temperature, and

superscripts s and b stand for surface and bulk, respectively.

For a pure liquid,

$$\mu_i^{0,s}(T,p) - \mu_i^{0,b}(T,p) = \gamma_i a_i \quad (2)$$

where  $\gamma_i$  is the surface tension of pure component  $i$ .

Substituting equation (2) into equation (1) gives

Butler's<sup>31</sup> equation for a perfect solution where  $a_i = a_j =$

a

$$\gamma = \gamma_i(T,p) + \frac{RT}{a_i} \ln \frac{x_i^s}{x_i^b} \quad (3)$$

For a two-component system  $(x_1 + x_2) = 1$  and

$$\gamma_1(T,p) + \frac{RT}{a} \ln \frac{x_1^s}{x_1^b} = \gamma_2(T,p) + \frac{RT}{a} \ln \frac{x_2^s}{x_2^b} \quad (4)$$

or rearranging,

$$\frac{x_1^b}{x_2^b} \frac{\exp(-\gamma_1 a/RT)}{\exp(-\gamma_2 a/RT)} = \frac{1}{x_2^s} - 1 = \frac{x_1^s}{x_2^s} \quad (5)$$

Solving for  $x_2^s$ , Schuchowitsky's<sup>32</sup> equation is produced

$$x_2^s = \frac{x_2^b \exp(-\gamma_2 a/RT)}{x_1^b \exp(-\gamma_1 a/RT) + x_2^b \exp(-\gamma_2 a/RT)} \quad (6)$$

Substituting equation (6) into equation (3) gives

Guggenheim's<sup>33,34</sup> equation

$$\exp(-\gamma a/RT) = x_1^b \exp(-\gamma_1 a/RT) + x_2^b \exp(-\gamma_2 a/RT) \quad (7a)$$

or

$$\gamma = -\frac{RT}{a} \ln[x_1^b \exp(-\gamma_1 a/RT) + x_2^b \exp(-\gamma_2 a/RT)] \quad (7b)$$

Extending the above general approach by taking non-ideality into account while retaining the assumption of equal molar areas for both components, equation (3) becomes<sup>35</sup>:

$$\gamma = \gamma_i(T,p) + \frac{RT}{a} \ln \frac{f_i^s x_i^s}{f_i^b x_i^b} \quad (8)$$

Where,  $f_i$  is the activity coefficient of component  $i$ .

If  $f_1^s = f_2^s = 1$ , then equation (7b) takes the form

$$\gamma = -\frac{RT}{a} \ln[f_1^b x_1^b \exp(-\gamma_1 a/RT) + f_2^b x_2^b \exp(-\gamma_2 a/RT)] \quad (9)$$

Prigogine and Marechal<sup>37,38</sup> have extended this approach to solutions of components of unequal surface areas and volumes by employing the Flory-Huggins theory of mixing. The surface is considered to be a monolayer containing monomers and  $r$ -mers lying parallel to the surface. For non-athermal solutions the results require the estimation of lattice coordination numbers. To simplify the

resulting surface tension expression, Gaines<sup>41</sup> proposed that the surface be considered ideal. For a two-component solution then

$$\begin{aligned}\mu_1^s &= \mu_1^{0,s}(T,p) + RT[\ln \phi_1^s + (\frac{r-1}{r})(1 - \phi_1^s)] - \gamma a \\ &= \mu_1^{0,b}(T,p) + RT[\ln \phi_1^b + (\frac{r-1}{r})(1 - \phi_1^s)] \\ &\quad + N\beta(1 - \phi_1)^2 = \mu_1^b\end{aligned}\quad (10)$$

and

$$\begin{aligned}\mu_2^s &= \mu_2^{0,s}(T,p) + RT[\ln \phi_2^s - (r-1)(1 - \phi_2^s)] - \gamma r a \\ &= \mu_2^{0,b}(T,p) + RT[\ln \phi_2^s - (r-1)(1 - \phi_2^s)] + \\ &\quad rN\beta(1 - \phi_2)^2 = \mu_2^b\end{aligned}\quad (11)$$

where,  $\phi_i$  = the volume fraction of component  $i$ ,

$r$  = the ratio of the molar volumes of components one and two,  $V_2/V_1$

$\beta$  = the interaction parameter, and

$a = V_1^{2/3} N^{1/3}$ , where  $N$  is Avagadro's number.

For the pure components

$$\mu_1^{0,s} - \mu_1^{0,b} = \gamma_1 a \quad \text{and} \quad \mu_2^{0,s} - \mu_2^{0,b} = r\gamma_2 a \quad (12)$$

Substituting equation (12) into equations (10)-(11) gives:

$$\gamma = \gamma_1 + \frac{RT}{a} \left[ \ln \frac{\phi_1^s}{\phi_1^b} + \left( \frac{r-1}{r} \right) (\phi_1^b - \phi_1^s) \right] - \frac{\beta N}{a} (\phi_2)^2 \quad (13a)$$

and

$$\gamma = \gamma_2 + \frac{RT}{ar} \left[ \ln \frac{\phi_2^s}{\phi_2^b} + (r-1)(\phi_2^s - \phi_2^b) \right] - \frac{\beta N}{a} (\phi_1)^2 \quad (13b)$$

The quantity  $\phi_1^s$  is required. Equation (13a) and (13b) may be equated and rearranged to give:

$$\frac{\phi_1^s}{(1 - \phi_1^s)^{1/r}} = \frac{\phi_1^b}{(1 - \phi_1^b)^{1/r}} \exp[(\gamma_2 - \gamma_1)a/RT] \exp\left(\frac{\beta N(1 - 2\phi_1^b)}{RT}\right) \quad (14)$$

The values of  $\phi_1^s$  and  $\phi_2^s$  may be therefore determined from experimental quantities and one adjustable parameter,  $\beta$ . Equation (14) has no analytic solution for arbitrary values of  $r$ .

These relationships indicate the problems which exist in attempting to model the concentration dependence of the surface tension of binary mixtures. A monolayer surface is assumed. This permits the use of a molecular surface area term which can be estimated from values derived from bulk systems. These estimates generally require an assumed geometry. For simplicity of calculation, the molecular surface area is also assumed to be independent of concentration. Surface non-ideality is also difficult to

quantitate. The number of nearest neighbors at the surface and the surface orientation of flexible chains are not known. For any but the perfect systems, the models are approximate and the relationships include adjustable parameters.

Recognizing the limitations of theory, this investigation has been limited to three simple and related systems. The surface and interfacial tensions of binary mixtures of benzene, toluene, and ethylbenzene with decane have been measured at air-liquid and water-liquid interfaces. These systems serve as models for the widely studied solubilization of aromatic hydrocarbons in lipid assemblies.

In this field much attention has been paid to mixtures of molten metals<sup>35</sup>, mixtures of liquified gases<sup>39</sup>, and aqueous polymer solutions<sup>41</sup>. Systems of similarly sized relatively spherical molecules have been examined to test the different models proposed. The aromatic-aliphatic systems have received comparatively little attention. Schmidt, Randall, and Clever<sup>42</sup> have reported a study of the surface tensions of benzene-hexane and benzene-dodecane systems at different temperatures. They attempted to fit their data to the equation of Hildebrand<sup>36</sup>, for ideally mixing molecules of unequal size. The molecular area of the aliphatic component was chosen as an adjustable parameter. The best fit value for hexane was close to that which could be approximated from a spherical model; the

dodecane value was from 3.5 to five times greater. Gaines<sup>43</sup> has applied his revised form of the Prigogine-Marechal equation (13) to the data of Schmidt et al. The best fit  $\beta$  interaction parameter was greater for the dodecane system than for the hexane system.

Aveyard<sup>44</sup> has compared the above athermal mixing relations to experimental data for the surface tension and interfacial tension against water of binary mixtures of aliphatic compounds. Better agreement was found for the surface tension than for the interfacial tension data. Aveyard and Haydon<sup>45</sup> have also demonstrated that the surface tension data of benzene-dibenzyl mixtures at 60°C reported by Kondo and Ono could be fitted by equation (13) with  $\beta = 0$  (athermal limit) across the whole composition range.

Handa and Mukerjee<sup>46</sup> have measured surface tensions and interfacial tensions against water of some alkane-perfluoroalkane mixtures. These systems are highly non-ideal and show deep minima in the surface tension vs. mole fraction composition curves. The results were compared with calculated values from the above relations. The Prigogine-Marechal equation was used with a fixed  $\beta$  parameter estimated from regular solution theory. No model was found to fit the data across the whole composition range.

Edmonds and McLure<sup>47</sup> have recently employed Gaines' equations to determine  $\beta$  values from the surface tensions of N-alkane-dimethyl siloxane mixtures. Although they

found the data could be fitted using an adjustable parameter, they have explained the model's success as "certainly to some extent the result of a fortuitous compensation of errors." They criticize the need for an adjustable parameter and the inability to assess the influence of chain flexibility.

### B. Scope and Aim

This study employs decane as a model aliphatic hydrocarbon to simulate the micellar core. The surface properties of binary decane-aromatic mixtures are examined. The simple aromatic series benzene, toluene, and ethylbenzene is used to examine the effects of aliphatic substituents. Since there are fewer nearest neighbors for each molecule to interact with at the surface, the deviations from ideality at the surface are expected to be smaller than in the bulk.<sup>48</sup> Since the surface tension values are determined from systems containing only two primary components, these results provide a test for the ability of the theoretical models to describe surface behavior. The perturbing effects of water on the interfacial properties of decane-aromatic binary mixtures can then be examined through comparison with the surface tension data. The interfacial tension data across the whole composition range are used to determine the adsorption of the aromatic component to the water-organic liquid surface. Using the bulk systems as

models, the distribution of the aromatic compounds between the decane-like micellar core and the micelle-water surface can be estimated.

## II. EXPERIMENTAL

A. Materials

Benzene (Aldrich Chem. Co., Gold Label 99+%)

Toluene (Aldrich Chem. Co., Gold Label 99+%)

Ethylbenzene (Aldrich Chem. Co., 99%)

Decane (Aldrich Chem. Co., Gold Label 99+%)

Distilled water was redistilled from alkaline permanganate solution.

B. Methods1. Purification methods

Ethylbenzene was redistilled in glass. All of the organic chemicals were passed through activated magnesium silicate (Florisol<sup>®</sup> 60-100 mesh; J. T. Baker) to remove polar contaminants.<sup>46,49</sup> The surface tension values agreed with literature values within experimental error (Table I).

2. Surface tension measurement

The drop volume technique was employed. An Agla<sup>®</sup> syringe<sup>52</sup> with a tip ground so as to produce a flat unbevelled surface was connected to a micrometer and fitted to a thermostatted container. The surface tension is related to the drop volume by equation (15).

Table I. Surface Tension Values at 25°C.

<u>Compound</u>	<u>Experimental</u>	<u>Literature</u>	<u>Ref.</u>
Benzene	28.31	28.22	50
		28.18	51
Toluene	27.88	27.92	50
		27.97	51
Ethylbenzene	28.41	28.48	51
		28.75	50
Decane	23.38	23.37	50

---

$$\gamma = \frac{V(\Delta\rho)g}{2\pi r} f \quad (15)$$

where,  $\gamma$  = the surface tension,

$V$  = the drop volume,

$\Delta\rho$  = the difference in density between the vapor and liquid phases and is approximated by the density of the liquid,

$g = 980 \text{ cm sec}^{-2}$ ,

$r$  = the radius of the syringe tip, and,

$f$  = a function of  $r$  and  $V^{1/3}$  and corrects for the deviation from sphericity of the drop formed on the syringe tip.

The function  $f$  was determined by interpolation from the tables of Harkins and Brown.<sup>53</sup> The radius of the tip was determined using the literature values for the surface tensions of water<sup>49</sup> and decane<sup>49</sup> in equation (1). Each value of surface tension reported is a mean of ten drops.

### 3. Interfacial tension measurements

Interfacial tension was measured by the Wilhelmy plate method. A Biolar<sup>®</sup> precision balance scaled in 0.2 mg divisions was employed. Typically, 50 ml of double-distilled water and 50 to 70 ml of organic phase were placed into a double-walled container connected to a thermostatted water bath. The two phases were agitated for

about 5 minutes and allowed to equilibrate for about 30 minutes. A clean platinum plate stored in chromic acid solution was washed with water and then dried over a flame. The dried plate was attached to one arm of the balance and immersed into the upper (organic) phase. The instrument was then adjusted so that the balance read zero when the plate was in the upper phase and wetted with the upper phase. The plate was then removed from the upper phase and cleaned with distilled acetone, allowed to air dry, immersed into chromic acid solution, washed with water, and wetted with water. The water-wetted plate was reattached to the balance. Since the plate was then heavier in the upper phase, a correction was made by adding weight to the balance. This adjustment was usually less than 10 mg, generally ranging from one to eight mg. The plate was then lowered to the oil-water interface at which point it was taken into the lower phase. By adding weight to the balance, the plate is raised from the lower phase and returned to the position it held before entering the lower phase. In other words the lower edge of the plate is at the oil-water interface. The force measured is that required to overcome the downward pull of interfacial tension.<sup>54</sup> The weight measured is that of the meniscus which has been pulled up above the mean level of the liquid surface.<sup>54</sup> The interfacial tension,  $\gamma$ , is the weight (= (mass)g) of the meniscus per unit length of perimeter (p)

of the plate:

$$\gamma = m g p^{-1} \quad (16)$$

Experimentally, the value of the perimeter was determined by taking an average value using pure liquid interfaces and the literature values for their interfacial tensions.

After reading the value of interfacial tension, a known amount of one organic component was added to the system and the complete process, including buoyancy correction, was repeated at the new concentration. In this manner the interfacial tension was measured over the entire composition range in three runs.

Although the container was covered with a plexiglas plate, an opening in the system must exist so that the Wilhelmy platinum plate could be connected to the balance. Evaporation was measured in two ways. The concentration of a 0.0047M solution of toluene in decane was measured spectrophotometrically and found not to change over a period of four hours. Also, a benzene system at 0.7088 mole fraction in decane was left for eleven hours. The interfacial tension change was less than  $0.2 \text{ dynes cm}^{-1}$ . An ethylbenzene system at 0.411 mole fraction in decane was left for three days with no change in interfacial tension.

At least five measurements with an initially wetted plate were carried out at each composition studied. In the

case of the ethylbenzene system, in a region where concentrations from two different dilution runs overlapped over a mole fraction range of about 0.1, good agreement was obtained. A few duplicate run measurements in the case of the benzene system also produced consistent results.

#### 4. Density determination

Density was measured using one ml and two ml capillary pycnometers. The method described by Bauer and Levin<sup>55</sup> was employed. The pycnometers were filled at room temperature, covered, and allowed to equilibrate in a 25°C water bath. After about 15 minutes in the bath, they were removed and the capillaries inserted. They were returned to the bath for a few more minutes and then dried and weighed. The flat top of the pycnometer was dried by touching quickly with lens paper, and then the sides were thoroughly wiped. Each density reading was a mean of three values. The pycnometers were calibrated with double-distilled water.

## III. RESULTS

The values of the surface tensions for the benzene-decane, toluene-decane, and ethylbenzene-decane mixtures at 25°C are listed in Tables II, III, and IV, respectively; and are presented graphically in Figures 1, 2, and 3, respectively. Using the drop-volume method, each value is a mean of ten drops. Replicate measurements on pure decane agreed to within  $\pm 0.05$  dynes  $\text{cm}^{-1}$ . When all of the data points were considered together, the mean deviations around smooth curves were less than  $\pm 0.1$  dynes  $\text{cm}^{-1}$ . Barring unknown systematic errors, the overall reliability of the data was estimated to be within  $\pm 0.1$  dynes  $\text{cm}^{-1}$ .

The values of the interfacial tensions of benzene-decane, toluene-decane, and ethylbenzene-decane mixtures against water at 25°C are listed in Tables V, VI, and VII, respectively; and are presented graphically in Figures 4, 5, and 6, respectively. The curves drawn in Figures 4, 5, and 6 are consistent with graphical integration of the derivative curves obtained for calculation of surface excess quantities to be discussed. At least five measurements using the Wilhelmy plate method were carried out at each composition studied. The values lay within 0.1 dyne  $\text{cm}^{-1}$  of the mean. From the mean deviations around smooth lines, the overall reliability of the data was estimated to be within  $\pm 0.2$  dynes  $\text{cm}^{-1}$ , if systematic error is

negligible.

The density values for benzene-decane, toluene-decane, and ethylbenzene-decane mixtures at 25°C are tabulated in Table VIII. One standard deviation was found to be no larger than 0.1% of the mean value. The experimentally determined densities of the pure liquids agree with literature values within  $\pm 0.13\%$ .

Table II. Surface Tensions of Benzene-Decane Mixtures  
Against Air at 25°C.

<u>Mole Fraction Toluene</u>	<u>Surface Tension/dynes cm<sup>-1</sup></u>
0.0	23.38
0.0427	23.44
0.099	23.49
0.1495	23.49
0.250	23.66
0.462	23.97
0.6125	24.33
0.800	25.44
0.900	26.52
1.00	28.31

---

Figure 1. Surface tensions of benzene-decane mixtures at 25°C plotted as a function of the mole fraction of benzene.

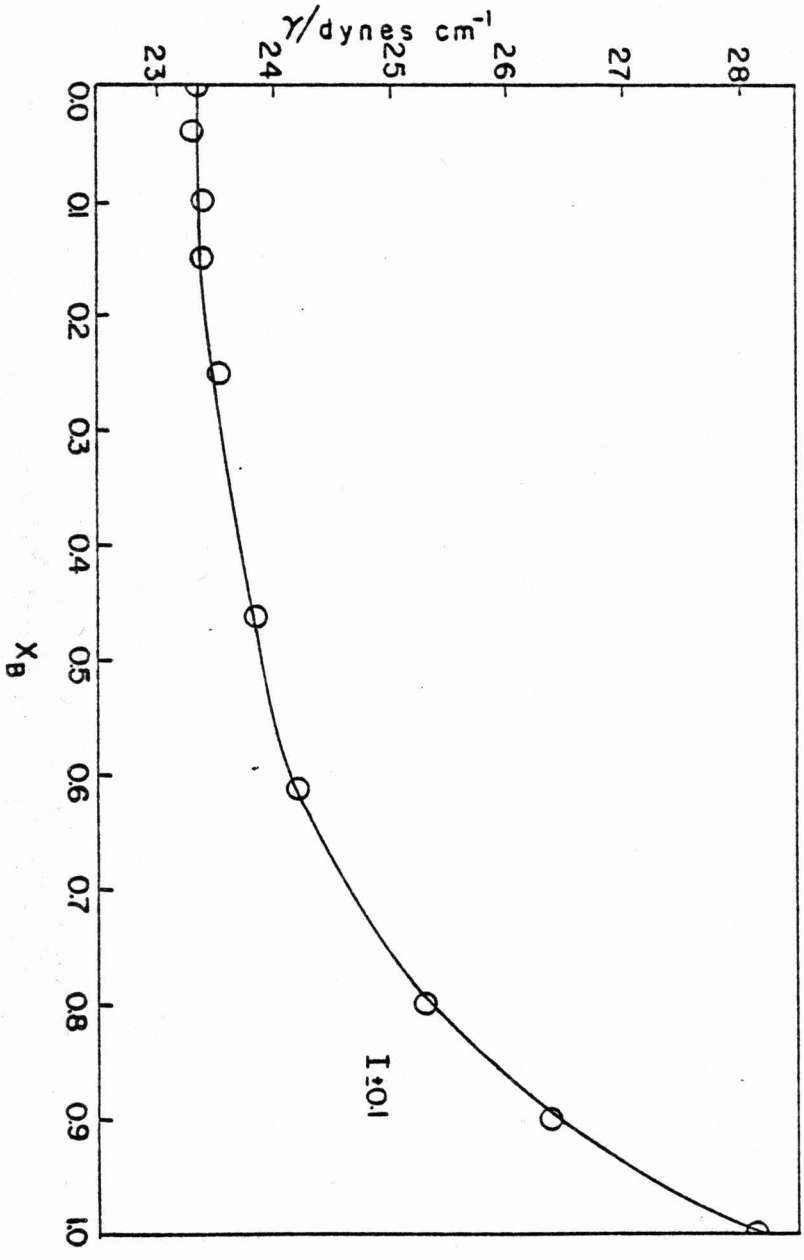


Table III. Surface Tensions of Toluene-Decane Mixtures  
Against Air at 25°C.

<u>Mole Fraction Toluene</u>	<u>Surface Tension/dynes cm<sup>-1</sup></u>
0.0	23.38
0.038	23.37
0.079	23.42
0.153	23.50
0.274	23.90
0.274	23.84
0.478	24.35
0.595	24.71
0.786	25.70
0.874	26.35
1.0	27.88

---

Figure 2. Surface tensions of toluene-decane mixtures at 25°C plotted as a function of the mole fraction of toluene.

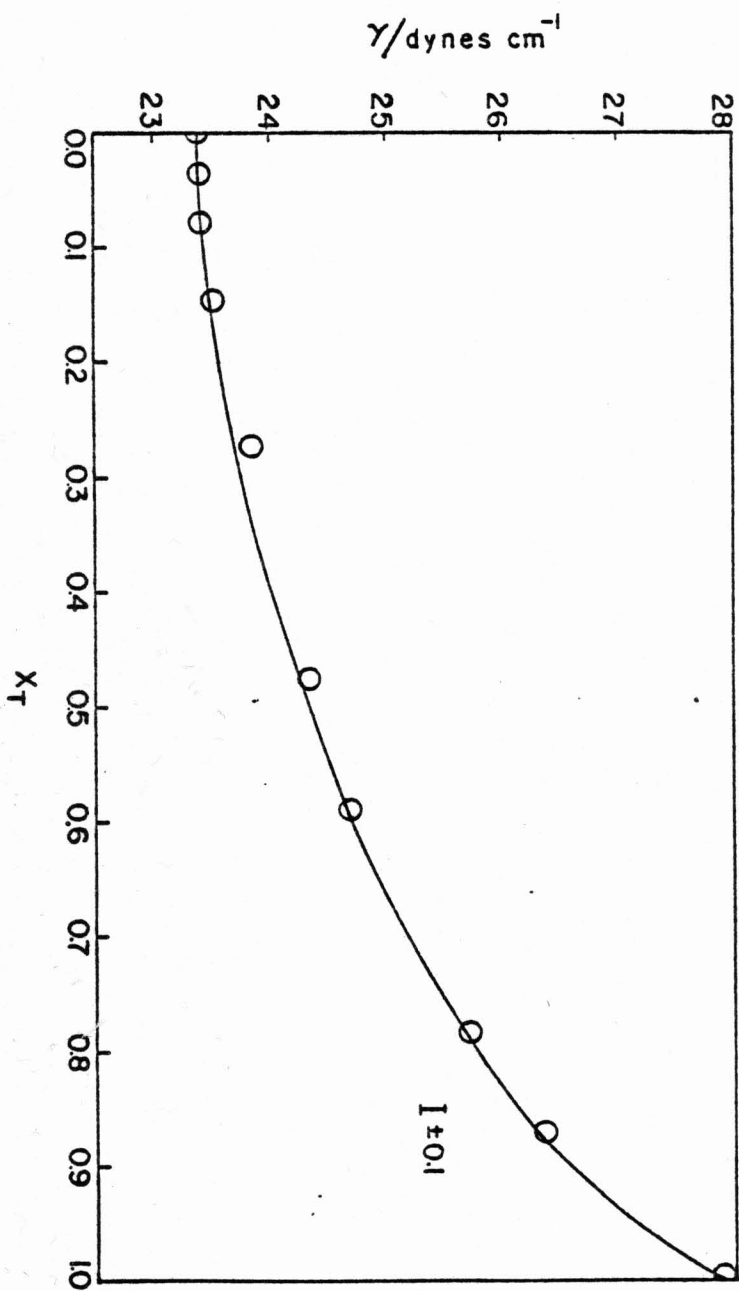


Table IV. Surface Tensions of Ethylbenzene-Decane Mixtures Against Air at 25°C.

<u>Mole Fraction Ethylbenzene</u>	<u>Surface Tension/dynes cm<sup>-1</sup></u>
0.0	23.38
0.042	23.46
0.085	23.52
0.153	23.68
0.253	23.93
0.445	24.53
0.601	25.14
0.800	26.17
0.899	27.16
1.0	28.41

---

Figure 3. Surface tensions of ethylbenzene-decane mixtures at 25°C plotted as a function of the mole fraction of ethylbenzene.

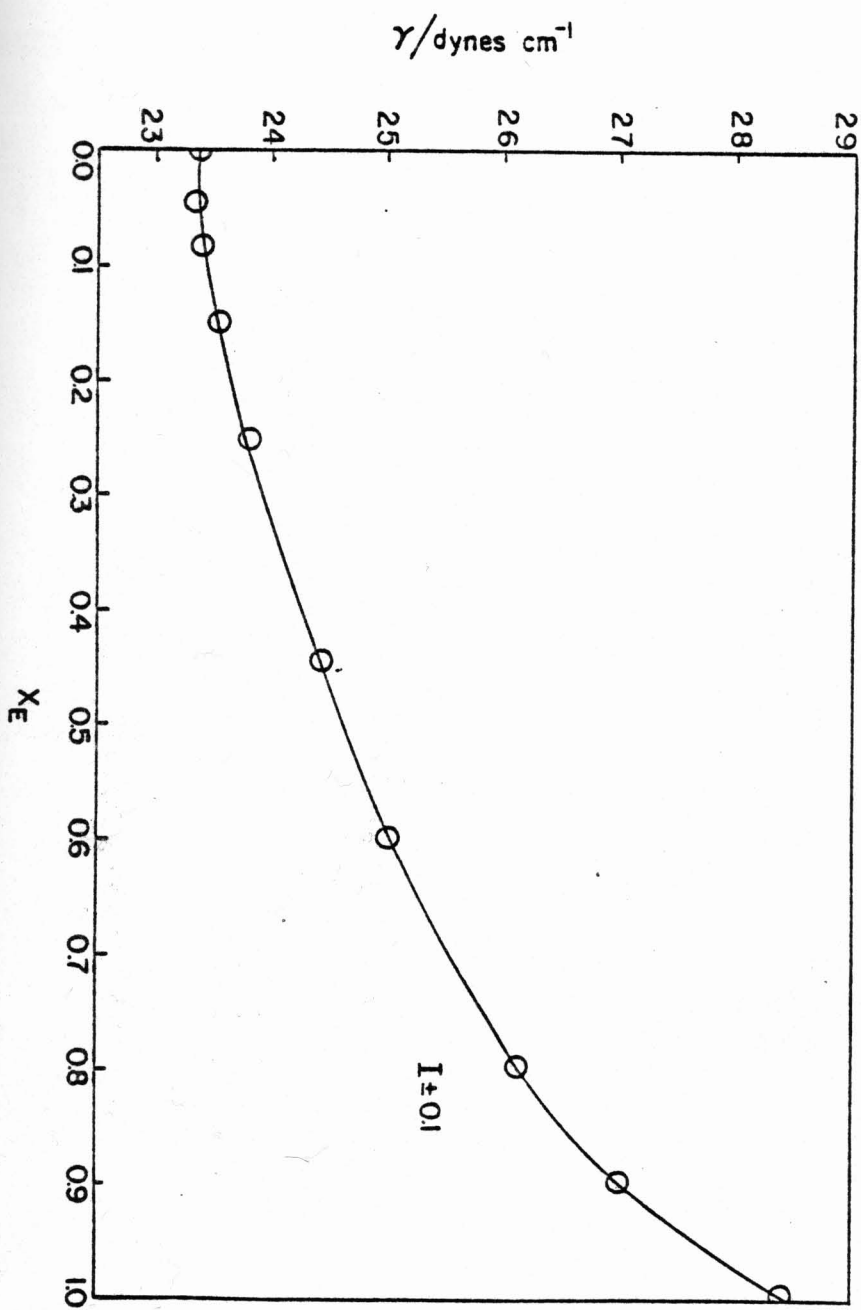


Table V. Interfacial Tensions of Benzene-Decane Mixtures  
Against Water at 25°C.

<u>Mole Fraction Benzene</u>	<u>Interfacial Tension/dynes cm<sup>-1</sup></u>	<u>S<sub>m</sub><sup>*</sup></u>
0.0	51.56 (51.7, ref. 24) (50.8, ref. 56)	0.011
0.0243	50.40	0.025
0.0474	49.73	0.020
0.0693	49.32	0.040
0.100	48.72	0.039
0.130	47.88	0.038
0.183	46.86	0.008
0.238	45.91	0.038
0.314	44.69	0.034
0.377	43.46	0.024
0.429	42.59	0.026
0.435	42.38	0.016
0.467	41.95	0.024
0.568	40.01	0.011
0.593	39.81	0.042
0.636	39.08	0.024
0.709	38.22	0.020
0.785	37.00	0.033
0.880	35.95	0.022
1.00	34.43 (34.0, ref. 57)	0.037

\*Standard deviation of the mean.

Figure 4. Interfacial tensions of benzene-decane mixtures against water plotted as a function of the mole fraction of benzene in the organic phase at 25°C.

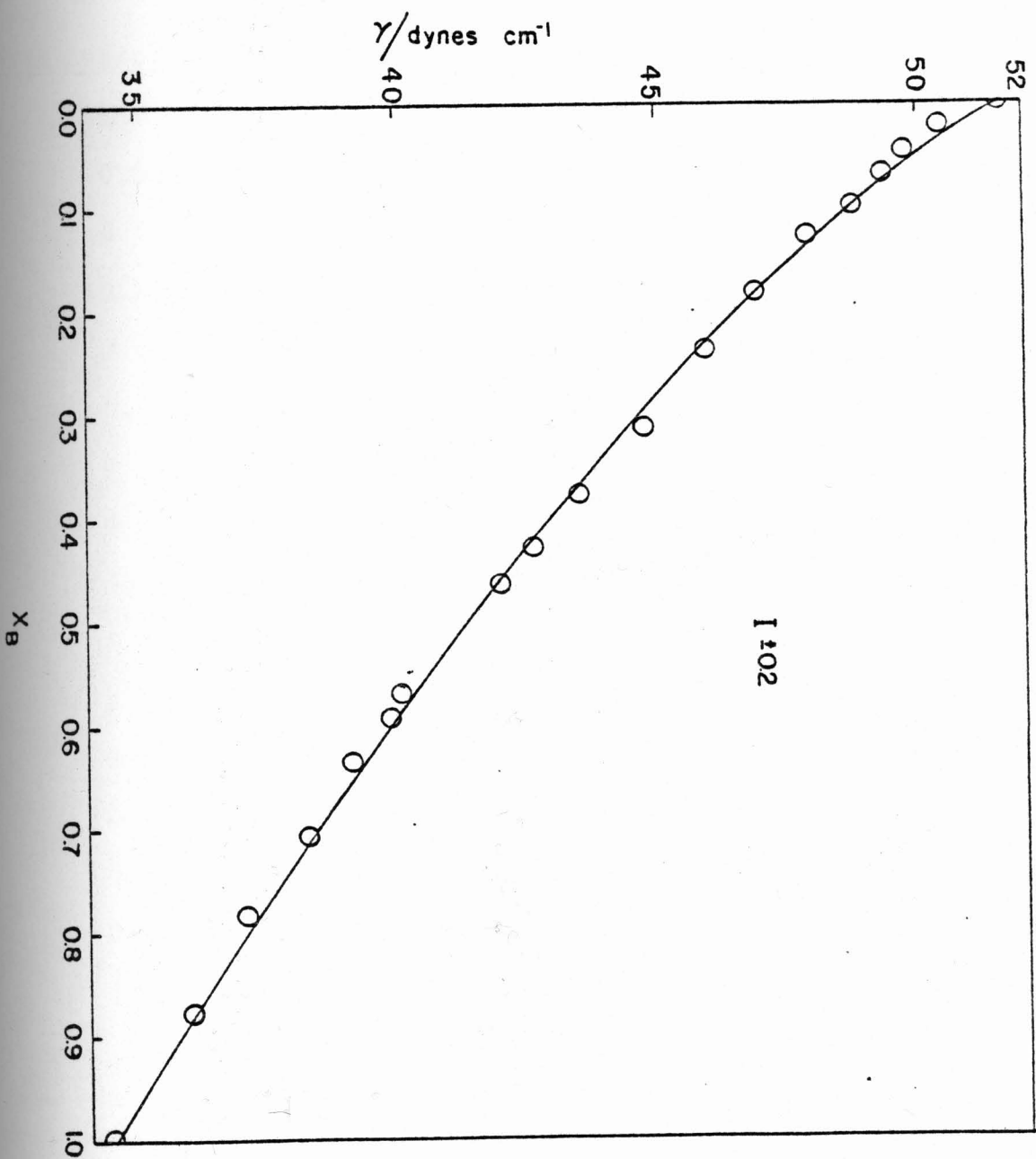


Table VI. Interfacial Tensions of Toluene-Decane Mixtures  
Against Water at 25°C.

Mole Fraction Toluene	Interfacial Tensions/dynes cm <sup>-1</sup>	S <sub>m</sub>
0.0	51.6*	0.037
0.0263	50.83	0.016
0.0512	50.34	0.023
0.0749	49.60	0.026
0.0975	48.95	0.012
0.139	47.95	0.013
0.222	46.22	0.023
0.355	43.76	0.007
0.423	42.92	0.014
0.478	42.08	0.007
0.524	41.42	0.018
0.595	40.3	0 <sup>a</sup>
0.645	39.53	0.016 <sup>b</sup>
0.811	37.86	0.014
0.865	37.04	0.026
0.928	36.36	0.013
1.00	35.70 (35.7, ref. 57)	0.009

\*For literature values see Table V.

<sup>a</sup>Only two readings taken.

<sup>b</sup>Only three readings taken.

Figure 5. Interfacial tension of toluene-decane mixtures against water plotted as a function of the mole fraction of toluene in the organic phase at 25°C.

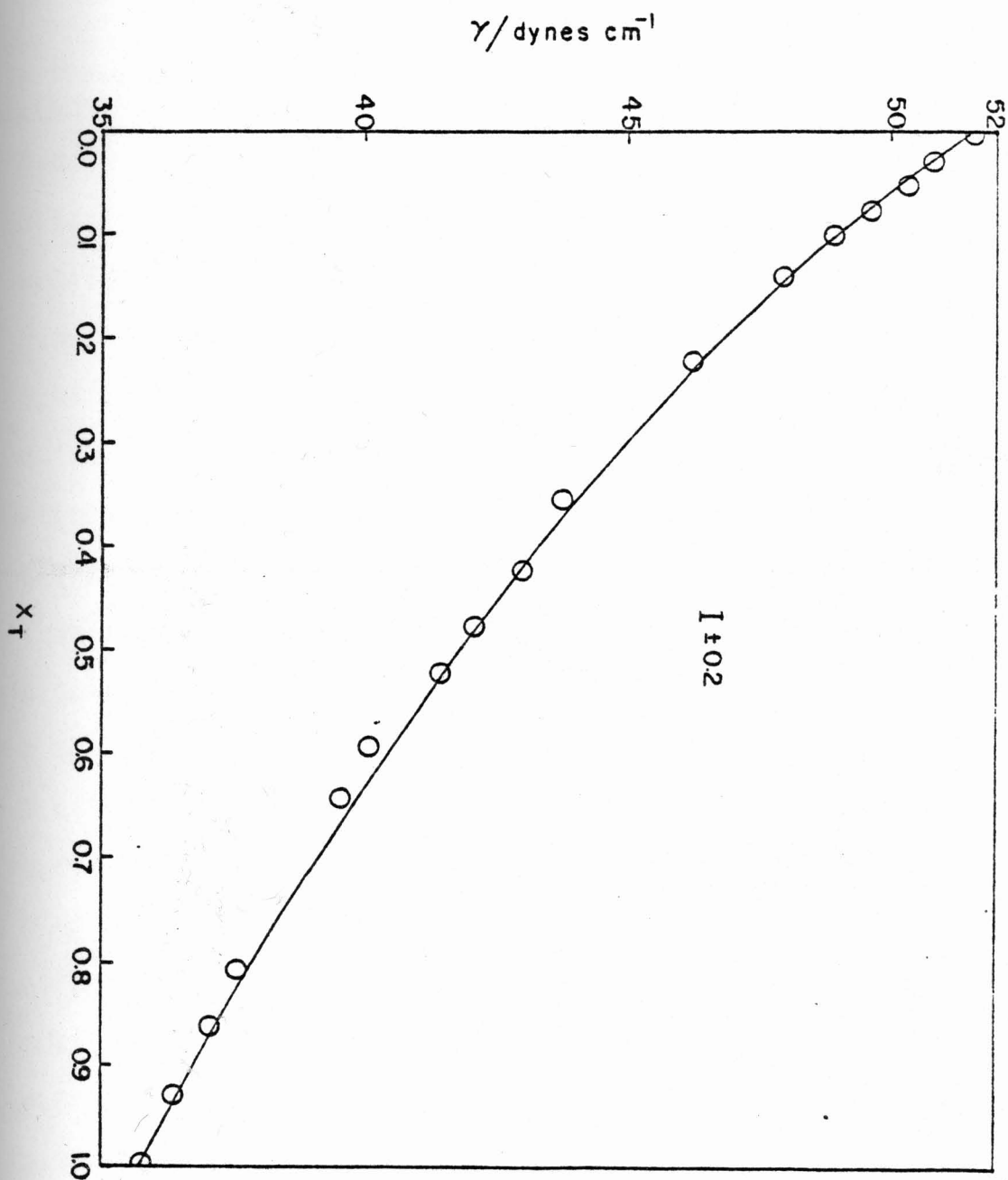


Table VII. Interfacial Tensions of Ethylbenzene-Decane  
Mixtures Against Water at 25°C.

<u>Mole Fraction Ethylbenzene</u>	<u>Interfacial Tension/dynes cm<sup>-1</sup></u>	<u>S<sub>m</sub></u>
0.0	51.52*	0.010
0.0234	50.57	0.013
0.0456	50.11	0.024
0.0668	49.82	0.0
0.0871	49.27	0.007
0.107	48.79	0.017
0.140	48.10	0.032
0.214	46.72	0.039
0.327	45.27	0.072
0.389	43.98	0.017
0.411	43.87	0.047
0.444	43.34	0.007
0.489	42.92	0.024
0.527	42.37	0.048
0.561	42.21	0.032
0.615	41.41	0.007
0.637	41.03	0.015
0.726	40.28	0.015
0.888	38.69	0.015
1.0	37.42 (37.4, ref. 57)	0.007

\*For literature values see Table V.

Figure 6. Interfacial tension of ethylbenzene-decane mixtures against water plotted as a function of the mole fraction of ethylbenzene in the organic phase at 25°C.

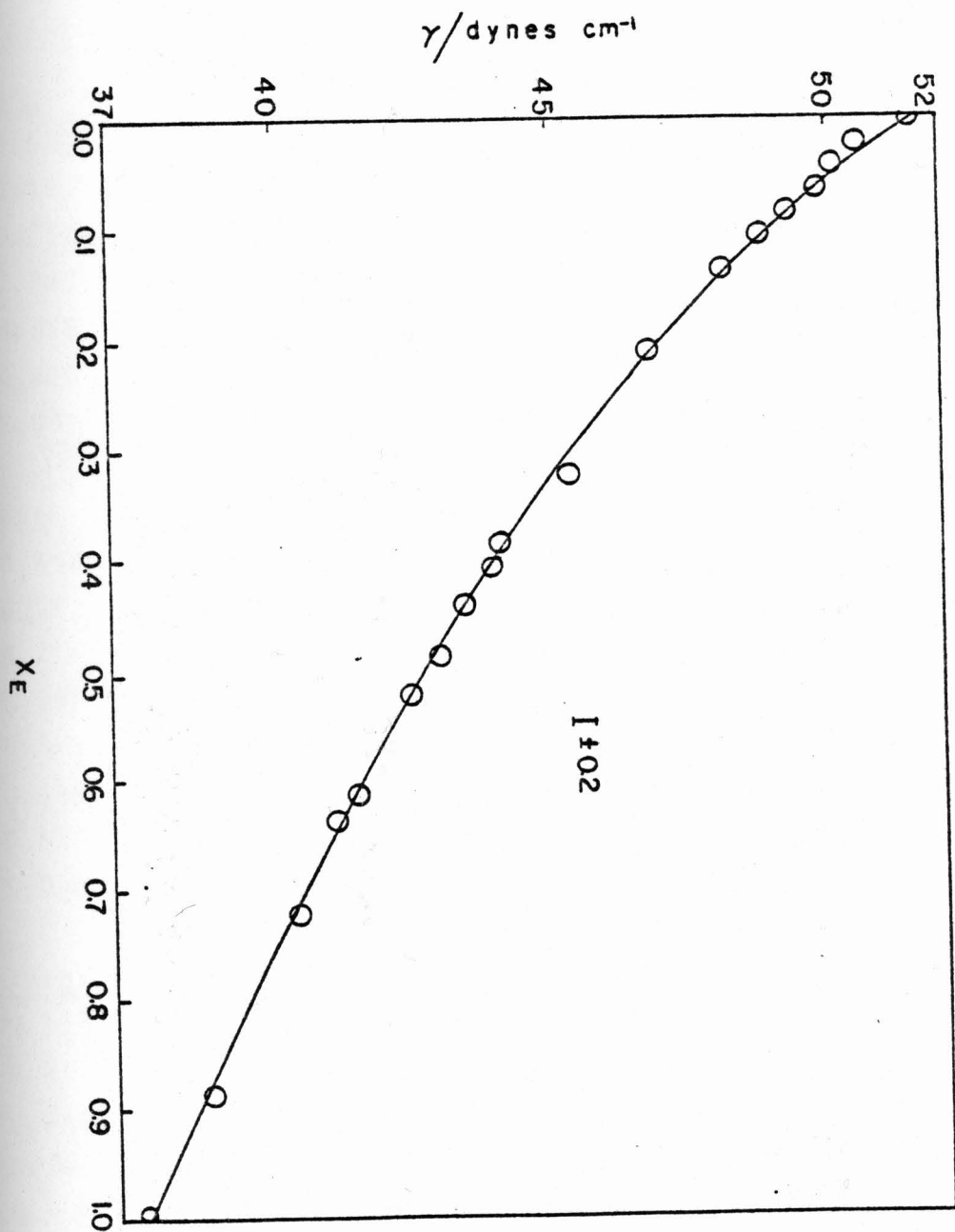


Table VIII. Densities of Benzene-Decane, Toluene-Decane, and Ethylbenzene-Decane Mixtures at 25°C.

<u>Mole Fraction</u>	<u>Density/(gm cm<sup>-3</sup>)</u>	<u>S<sub>m</sub></u>
<u>Benzene</u>		
0.0	0.7259 (0.7262, ref. 51)	0.0000577
0.150	0.7350	0.0000958
0.250	0.7431	0.000197
0.463	0.7616	0.000554
0.613	0.7801	0.0000958
0.800	0.8156	0.0001707
1.00	0.8726 (0.8737, ref. 51)	0.0003285
<u>Toluene</u>		
0.145	0.7365	0.000160
0.153	0.7372	0.000208
0.274	0.7478	0.0001767
0.293	0.7495	0.000208
0.478	0.7691	0.000260
0.696	0.7985	0.0000664
0.849	0.8258	0.0000577
1.000	0.8612 (0.8623, ref. 51)	0.0000577
<u>Ethylbenzene</u>		
0.153	0.7398	0.000192
0.253	0.7486	0.0000289
0.441	0.7708	0.0003614
0.601	0.7896	0.000173
0.800	0.8218	0.000202
1.00	0.8624 (0.86264, ref. 51)	0.000410

## IV. DISCUSSION

A. Surface Tensions

In order to compare the values calculated from theories of surface tension and the values determined experimentally, the surface tension data have been recalculated as excess quantities,  $\gamma^E = \gamma - \gamma_1 x_1 - \gamma_2 x_2$ . The excess surface tension vs. composition diagrams for binary mixtures of benzene, toluene, or ethylbenzene with decane are shown in Figures 7, 8, and 9, respectively. Since such data and graphs magnify errors and deviations, they are particularly useful for assessing the relative experimental errors and agreement with theory.<sup>42,47</sup>

The curves in Figures 7, 8, and 9 represent values predicted from several theories of surface tension of increasing complexity. Model A<sup>35</sup> employs equation (7b) (reproduced below for convenience) based on the simplest approach of perfect mixing of equally sized molecules.

$$\gamma = - \frac{RT}{a} \ln[x_1 \exp(-a\gamma_1/RT) + (1 - x_1)\exp(-a\gamma_2/RT)] \quad (7b)$$

Here  $a$  is taken as the arithmetic mean molar area. As can be seen in Figures 7, 8, and 9, the predicted values of  $\gamma^E$  are much higher than those observed in each case. The asymmetry of the experimental data is not reproduced either. Thus this very simple model appears to be inadequate.

Figure 7. Excess surface tensions,  $\gamma^E (= \gamma - \gamma_1 x_1 - \gamma_2 x_2)$ , of benzene-decane mixtures plotted as a function of the mole fraction of benzene at 25°C.

Open circles - experimental points

A - calculated values from equation 7

B - calculated values from equation 9

C - calculated values from equation 17

D - calculated values from equation 13

with  $\beta N = 126$  cal/mole (or

$\beta = 0.214$  kT)

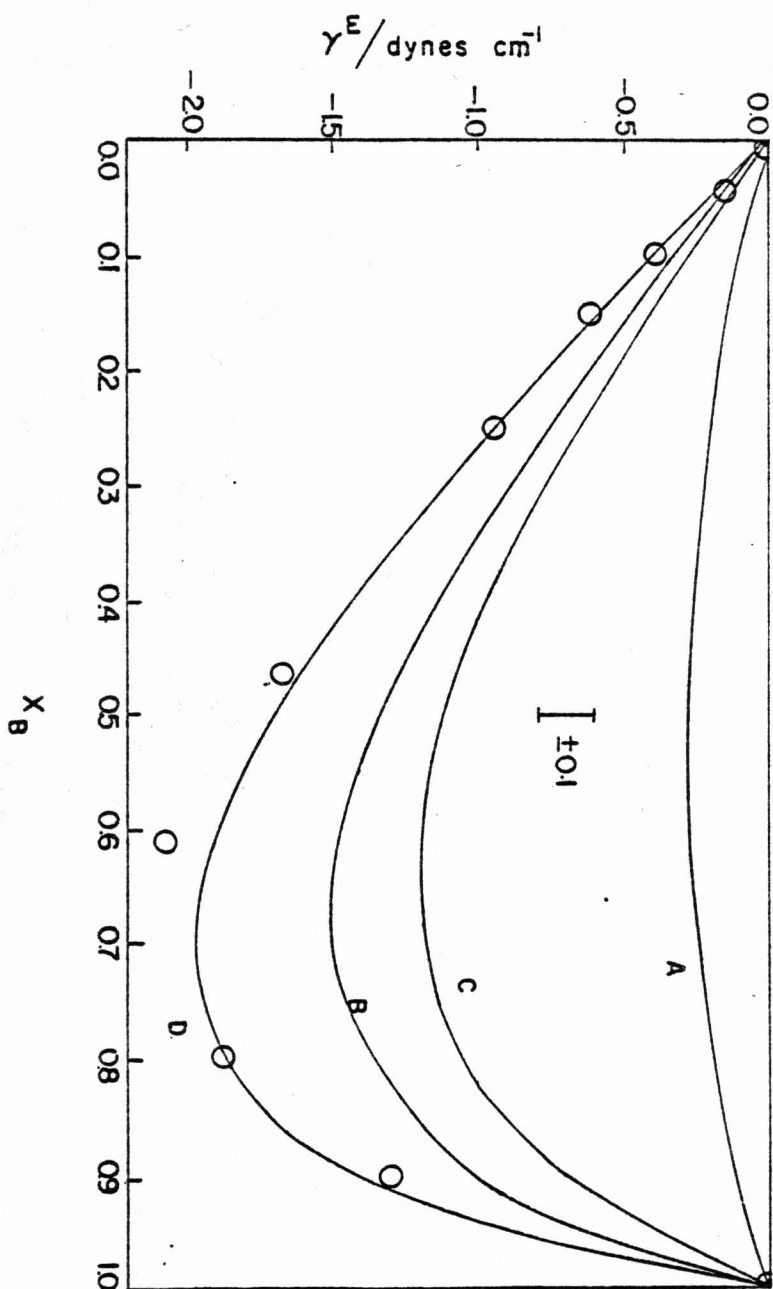


Figure 8. Excess surface tensions of toluene-decane mixtures plotted as a function of the mole fraction of toluene at 25°C.

Open circles - experimental points

A - calculated values from equation 7

B - calculated values from equation 9

C - calculated values from equation 17

D - calculated values from equation 13

with  $\beta N = 80$  cal/mole (or

$\beta = 0.135$  kT)

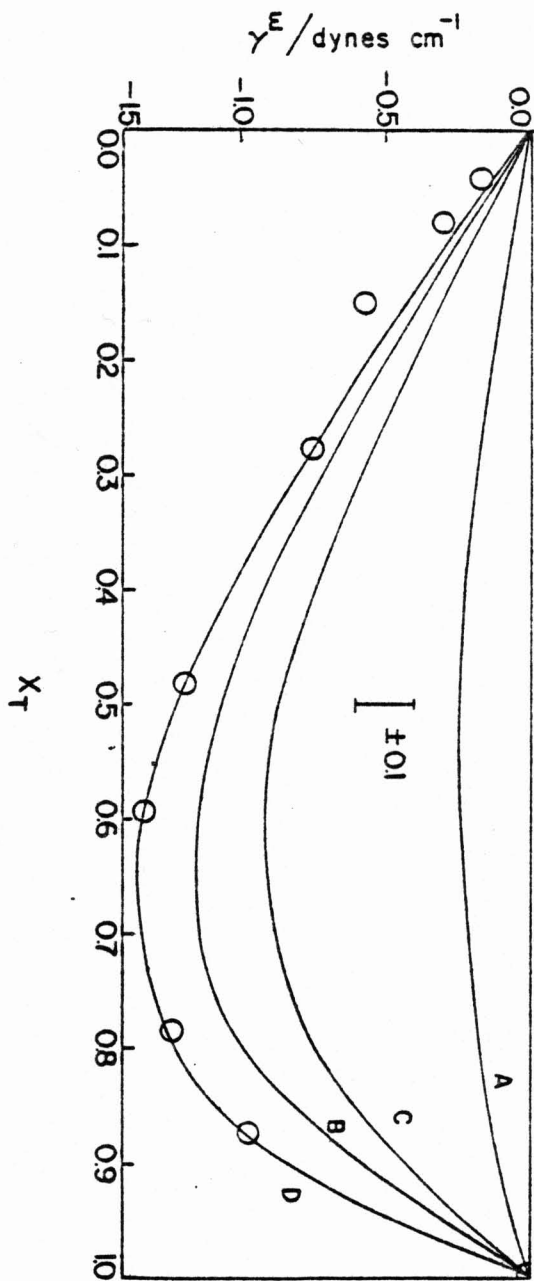


Figure 9. Excess surface tensions of ethylbenzene-decane mixtures plotted as a function of the mole fraction of ethylbenzene at 25°C.

Open circles - experimental points

A - calculated values from equation 7

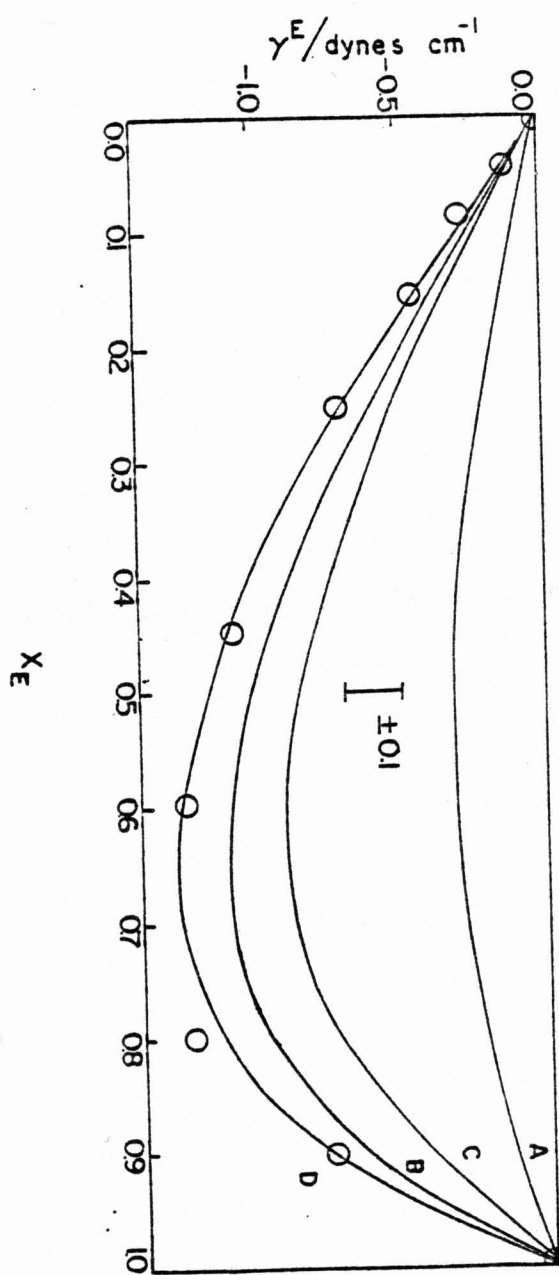
B - calculated values from equation 9

C - calculated values from equation 17

D - calculated values from equation 13

with  $\beta N = 76$  cal/mole (or

$\beta = 0.129$  kT)



An activity coefficient based upon the non-idealities occurring in the bulk may be included in equation (7b) resulting in equation (9) (reproduced below for convenience).

$$\gamma = - \frac{RT}{a} \ln [f_1 x_1 \exp(-a\gamma_1/RT) + f_2(1 - x_1)\exp(-a\gamma_2/RT)] \quad (9)$$

Experimental activity data were not available. The activity coefficients predicted from solubility parameter theory were used. Data on the N-octane-benzene system at this temperature indicated that solubility parameter theory could predict the activity coefficient to within 10% at infinite dilution.<sup>58</sup> The activity coefficient predicted by solubility parameter theory<sup>59</sup> can be expressed as:

$$f_i = \exp[V_i A_{ij}(1 - \phi_i)^2/RT]$$

where  $V_i$  is the molar volume of component  $i$ , and  $A_{ij}$  is the interaction parameter defined as

$$\left[ \left( \frac{\Delta E_{VAP,i}}{V_i} \right)^{1/2} - \left( \frac{\Delta E_{VAP,j}}{V_j} \right)^{1/2} \right]^2$$

Model B in Figures 7, 8, and 9 shows calculations based on this theory. The agreement with experimental data is much better than for the calculations based on equation (7b).

In particular the asymmetry of the  $\gamma^E - x$  curve is reproduced well. The agreement with experimental data is not quantitative, however. The reasons for the discrepancies include the inadequacies of the solubility parameter theory for predicting bulk activity coefficients, the assumption of an ideal surface, and the choice of the mean size.

In order to examine the importance of the differences in sizes of the two components, the Flory-Huggins theory<sup>37</sup> of mixing can be used. Model C employs equation (17)

$$\gamma = \gamma_1 + \frac{RT}{a} \left[ \ln\left(\frac{\phi_1^s}{\phi_1}\right) + \left(\frac{r-1}{r}\right)(\phi_1 - \phi_1^s) \right] \quad (17)$$

Although this approach assumes athermal mixing, the asymmetric nature of the  $\gamma^E - x$  curves is reproduced. However, the agreement with experimental data is poorer than seen for model B.

For a realistic physical description of these systems, non-ideality effects both in the bulk solutions and at the surface, as well as size differences, must be invoked. A completely general approach would require the inclusion of many adjustable parameters. A reasonable compromise has been suggested by Gaines. Using a single interaction parameter  $\beta$ , the surface tension can be expressed by equation (13) (reproduced below for convenience):

$$\gamma = \gamma_1 + \frac{RT}{a} \left[ \ln \left( \frac{\phi_1^s}{\phi_1} \right) + \left( \frac{r-1}{r} \right) (\phi_1 - \phi_1^s) \right] - \frac{\beta}{a} (1 - \phi_1)^2 \quad (13)$$

Model D in Figures 7, 8, and 9 is based on this equation. The value of  $\beta$  used in each figure is the average of five  $\beta$  values estimated at five different concentrations. Model D fits the experimental data within experimental error over the whole composition range in all three systems. Although the  $\beta$  parameter is an adjustable parameter in this theory, and, therefore, better fits might be expected than for the other theories, the magnitude of  $\beta$  suggests that this theory is likely to be the most physically realistic, also. For example, model B could fit the data better if larger values for the activity coefficients had been used. However, the very significant effect of volume differences shown by model C suggests that such a fit of model B would be physically less meaningful than those given by the more comprehensive model D.

Effective  $\beta$  values for surface tension data for several systems including those systems studied here are shown in Table IX. Solubility parameter theory provides an interaction parameter calculated from bulk properties.  $A_{12}$  is based upon the relative tendencies of molecules to leave the bulk. The  $V_1$  term makes this parameter dimensionally comparable with  $\beta$ .  $V_1$  is used since it represents the

Table IX. Comparison of Interaction Parameters Determined from Solubility Parameter Theory and  $\beta$  Values from Air-Liquid Surface Tension Data.

System	$V_1 A_{12}/(\text{cal mole}^{-1})$	$\beta N/(\text{cal mole}^{-1})$
Benzene-Decane	181	126
Toluene-Decane	150	80
Ethylbenzene-Decane	143	76
Benzene-Hexane <sup>43</sup>	324	72
Benzene-Dodecane <sup>43</sup>	116	165

solvent-sized (aromatic-sized) molar volume upon which Flory-Huggins lattice theory is based. The best fitted values of  $\beta$  are indeed found to be less than those determined from solubility parameter theories in most cases. It should be noted that the neglect of surface non-ideality effects should reduce the "effective" non-idealities of bulk solutions required for fitting surface tension data. This is consistent with some cancellation of bulk non-ideality effects by surface effects.<sup>48</sup> The one exceptional case of the benzene-dodecane mixture and the opposite trend of  $\beta$  vs.  $V_1 A_{12}$  as alkyl chain length is increased in the benzene-n-alkane systems will require further examination. For the systems of interest, model D, then, provides a reasonable means for describing the surface tension data in a manner consistent with models for physical surfaces.

#### B. Interfacial Tension Studies

In Figures 10, 11, and 12, the interfacial tension data are plotted as excess quantities. Also shown are the theoretical predictions from some of the models mentioned. Model A calculations based on equation (7), which assumes perfect mixing of equally sized molecules, show minima in  $\gamma^E$  which are deeper than shown by the experimental data. Although not shown, taking activity coefficients into account (equation (9)) decreases calculated values of  $\gamma^E$  further, as expected. However, the discrepancy with

Figure 10. Excess interfacial tensions of benzene-decane mixtures against water plotted as a function of benzene in the organic phase at 25°C.

Open circles - experimental points

A - calculated from equation 7

C - calculated from equation 17

(points calculated denoted by x)

D - calculated from equation 13

with  $\beta N = 309$  cal/mole (or

$\beta = 0.523$  kT)

D' - calculated from equation 13

- with  $\beta N = 200$  cal/mole (or

$\beta = 0.337$  kT)

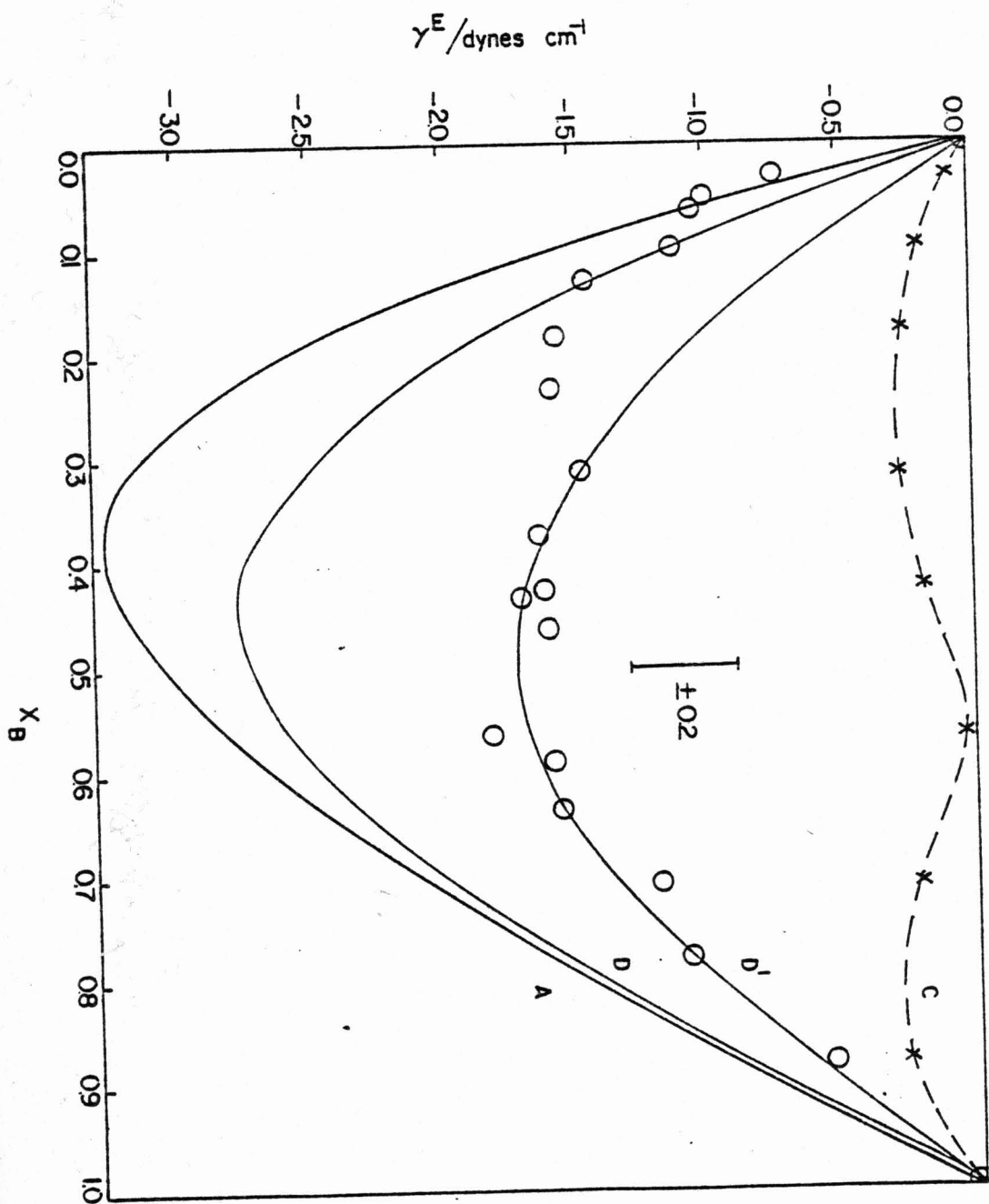


Figure 11. Excess interfacial tensions of toluene-decane mixtures against water at 25°C plotted as a function of the mole fraction of toluene in the organic phase at 25°C.

Open circles - experimental points

A - calculated from equation 7

C - calculated from equation 17

(points calculated denoted by x)

D - calculated from equation 13

with  $\beta N = 239$  cal/mole (or  
 $\beta = 0.404$  kT)

D' - calculated from equation 13

with  $\beta N = 173$  cal/mole (or  
 $\beta = 0.293$  kT)

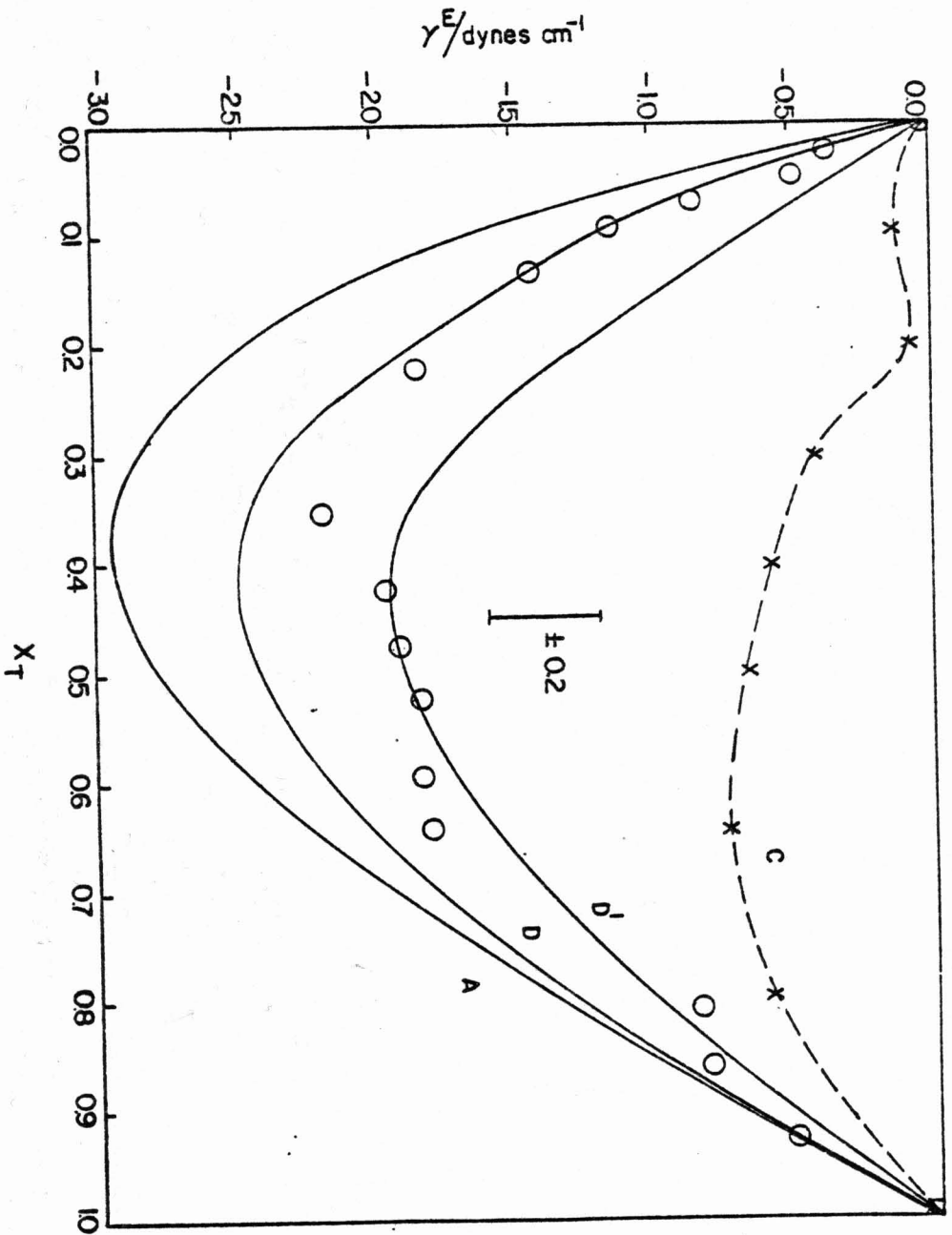


Figure 12. Excess interfacial tensions of ethylbenzene-decane mixtures against water at 25°C plotted as a function of the mole fraction of benzene in the organic phase.

Open circles - experimental points

A - calculated from equation 7

C - calculated from equation 9

(points calculated denoted by x)

D - calculated from equation 13

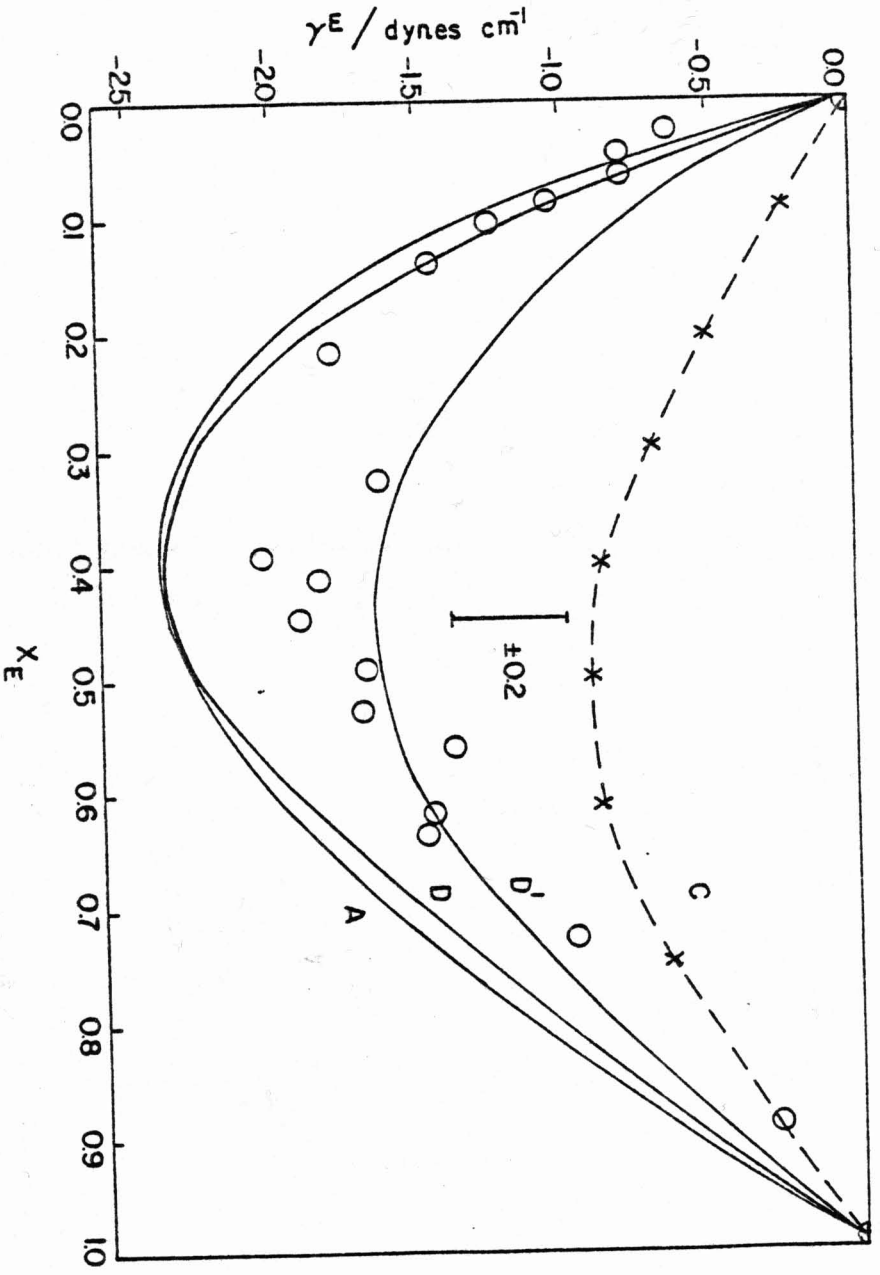
with  $\beta N = 217$  cal/mole (or

$\beta = 0.368$  kT)

D' - calculated from equation 13

with  $\beta N = 114$  cal/mole (or

$\beta = 0.193$  kT)



experimental data increases. These apparently unusual observations appear to be due to a switch in the ratios of the pure liquid tensions of molecules of different sizes. For surface tension data the larger species, decane, has the lower  $\gamma$  value. In the case of interfacial tension data, this is reversed. As a result, when mean "a" values are used in equations (7) and (9) the pure liquid tensions are weighted differently than they would have been had a values reflecting size differences been used.

In order to examine the effect of size differences, the Prigogine-Marechal equation (17) for athermal solutions was used.  $\gamma^E$  values calculated in this manner are denoted as model C in Figures 10, 11, and 12. The  $\gamma^E$  values are much less negative than predicted by models A and B, and a small unexpected maximum in the  $\gamma^E$  is observed for benzene and toluene. This relationship predicts much higher values for the interfacial tension than observed. The calculated values move closer to the experimental values in proceeding from benzene to toluene to ethylbenzene as in the case of the surface tension data. Notably, though, the minima in  $\gamma^E$  become deeper as the alkyl substituent is lengthened, which is the reverse of the trends with both the surface tension predictions of model C and the predicted values from models A and B for the interfacial tension. The changes in the relative size of the more surface active component as the interface is changed from air to water are responsible for

these effects.

Model D, the most comprehensive model which fitted surface tension data well using one adjustable parameter over the whole composition range, does not fit the interfacial tension data over the whole composition range. Curves marked D in Figures 10, 11, and 12 were drawn using the  $\beta$  value determined from data points close to  $x = 0.1$ . Curves marked D' were drawn for the benzene-decane-water system by averaging the  $\beta$  values determined from the experimental curve drawn at  $x_B = 0.354, 0.484, 0.594, 0.687$ . For toluene and ethylbenzene the interfacial tension value taken from the experimental curves at 0.5 volume fraction were used to calculate  $\beta$  for curve D' as suggested by Gaines.<sup>41</sup> It is clear that a single  $\beta$ -parameter is inadequate for interfacial tension data in contrast to the surface tension data. Significantly higher values of  $\beta$  are needed for the lower concentrations of the aromatic solutes, as indicated in Table X.

In order to examine the differing effects of air and water on the surface properties of these organic liquid mixtures, the significance of  $\beta$  must be considered again. In model D, the surface is assumed to be formally ideal. Therefore,  $\beta$  primarily originates with the organic liquid interactions. Water should have little effect on these bulk interactions due to its low solubility in the organic phase. However, as discussed before, the  $\beta$ -parameters

Table X. Comparison of  $\beta$  Values from Air-Liquid Surface Tension and Water-Liquid Interfacial Tensions.

System	Surface Tension $\beta N/(\text{cal mole}^{-1})$	Interfacial Tension $\beta N/(\text{cal mole}^{-1})$	
Benzene-Decane	126	310	$(x_B = 0.10)$
		200	$(0.354 \leq x_B \leq 0.687)$
Toluene-Decane	80	239	$(x_T = 0.0975)$
		173	$(x_T = 0.647)$
Ethylbenzene-Decane	76	218	$(x_E = 0.0871)$
		114	$(x_E = 0.614)$

required to fit surface or interfacial tension data are effective or net parameters for the whole system and combine or cancel at least elements of the non-idealities in the bulk and at the surface. Table X shows that the  $\beta$  determined from the interfacial tension data ( $\beta_{I.T.}$ ) is greater than the parameter determined from surface tensions ( $\beta_{S.T.}$ ) for all three systems. This means that the interfacial tension value for all mixtures is lower than would have been predicted on the basis of the interaction parameter determined from surface tension. The lower surface tension components, the aromatics, adsorb to the water-liquid surface to a greater extent relative to decane than would have been expected from interpretation of air-liquid surface tension results. The  $\beta_{I.T.}$  must then refer to some other effects beyond the non-specific dispersive interactions which are the major forces determining  $\beta_{S.T.}$ . Aromatic compounds are capable of acting as hydrogen bond acceptors through their ring systems.<sup>60,21</sup> Indeed, aromatic hydrocarbons are significantly more hydrophilic than aliphatic hydrocarbons, as can be seen from the differences in their aqueous solubilities.<sup>61</sup> Thus, at the water-liquid interface the relative adsorption of aromatics may be expected to be larger than predicted by  $\beta_{S.T.}$  due to specific hydrogen bonding interactions.

As mentioned above, the results also show that  $\beta$  changes with composition for the water-liquid systems and

that  $\beta$  decreases with increasing aromatic component composition in the mixture. Since hydrogen bonding interactions have a directional character<sup>62</sup>, a planar orientation of the aromatic ring at the water-liquid interface will allow H-bonding of the  $\pi$ -system and water.<sup>60</sup> In dilute benzene solutions, when few benzene molecules are at the surface, such planar orientations should be more likely to occur than at high surface concentrations when aromatic molecules in close contact can interact with each other. Therefore, to the extent that directional hydrogen bonding is responsible for adsorption of aromatics to the water-liquid surface, the tendency of aromatics to adsorb will be most fully expressed in dilute solution. The interfacial tension therefore falls rapidly with aromatic concentration and the fitted  $\beta$  value is consequently high in the dilute region. Model D calculations indicate that when  $x_B \approx 0.45$  ( $\phi_B \approx 0.3$ ), the  $\phi_B^S$  is greater than 0.7 for the water-decane-benzene system. The interface is much like that of a benzene-water interface, and, therefore,  $\beta$  is lower due to the high concentration of the more hydrophilic component at the surface. Specific hydrogen bonding interactions play a smaller role in lowering the interfacial tension at high aromatic concentration and, therefore, the  $\beta_{I.T.}$  values are closer to  $\beta_{S.T.}$  values.

A rigorous analysis of the Prigogine-Marechal parallel layer model of a monolayer interface indicates a

concentration dependence of  $\beta$  which is qualitatively consistent with the variation noted here. However, such an approach may be inappropriate here since the interactions with a third component at the interface are not accounted for in this model derived for analysis of surface tension data. Further investigation of the usefulness of the Prigogine-Marechal model for liquid-liquid interfaces of three component systems deserves future attention.

The decrease in the effective  $\beta_{I.T.}$  value with increasing alkyl substitution on the aromatic ring is consistent with the above explanation of results. The dispersive interactions between decane and the aromatic compound become more favorable with increasing alkyl chain length as shown by  $\beta_{S.T.}$ . Any differences in the hydrogen bonding abilities of these three aromatic compounds cannot be demonstrated through one adjustable interaction parameter.

In summary, although model D may be physically unrealistic since a monolayer of molecules is considered to be parallel to the surface and flexibility is not taken into account, this model provides a first attempt at assessing the interactions occurring in a system of molecules of differing sizes. The single adjustable interaction parameter provides a means to compare the interactions occurring in different systems. Since no suitable interaction parameter was found to fit the interfacial tension data across the

whole composition range, alternative means of assessing adsorption would be necessary.

Because of the availability of surface and interfacial tension data on the same organic liquid mixtures, it is possible to calculate the initial spreading coefficient,  $S$ , and the effect of the organic liquid composition on  $S$ . The initial spreading coefficient is defined as the difference between the work of adhesion and the work of cohesion<sup>63</sup>.

$$S_{i/j} = \gamma_j - (\gamma_i + \gamma_{ij}) \quad (18)$$

where,  $S_{i/j}$  is the spreading coefficient of  $i$  on  $j$ , and  $\gamma_{ij}$  is the interfacial tension of liquid  $i$  against liquid  $j$ . Figure 13 is a plot of calculated  $S$  values for spreading of three decane-aromatic mixtures on water. Notably, the initial spreading coefficient has a maximum at about 0.90 mole fraction of benzene. The height of the maximum is decreased in the case of toluene. For ethylbenzene  $S$  is nearly constant in the region around  $x_E = 0.90$ . The value of the initial spreading coefficient decreases with increasing alkyl substitution.

Figure 14 compares the experimentally determined initial spreading coefficient with the  $S$  values predicted from different models. The perfect mixing model<sup>35</sup> (equation (7)) and the Prigogine-Marechal athermal mixing model<sup>37</sup> (equation (17)) do not predict the maximum which

Figure 13. Initial spreading coefficients,  $S$ , of benzene-decane, toluene-decane, and ethylbenzene-decane mixtures on water at 25°C plotted as a function of the mole fraction of aromatic in the binary mixture.

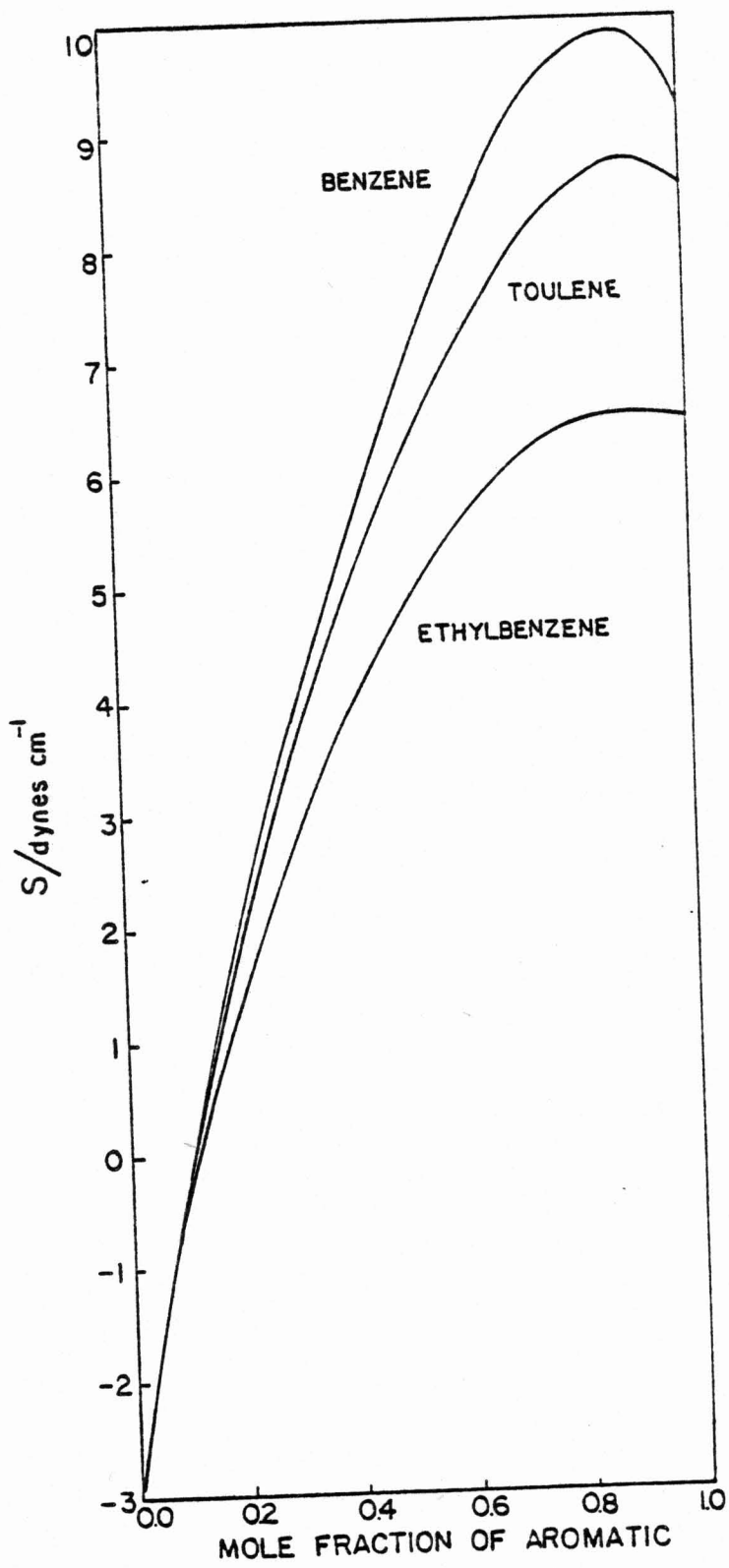


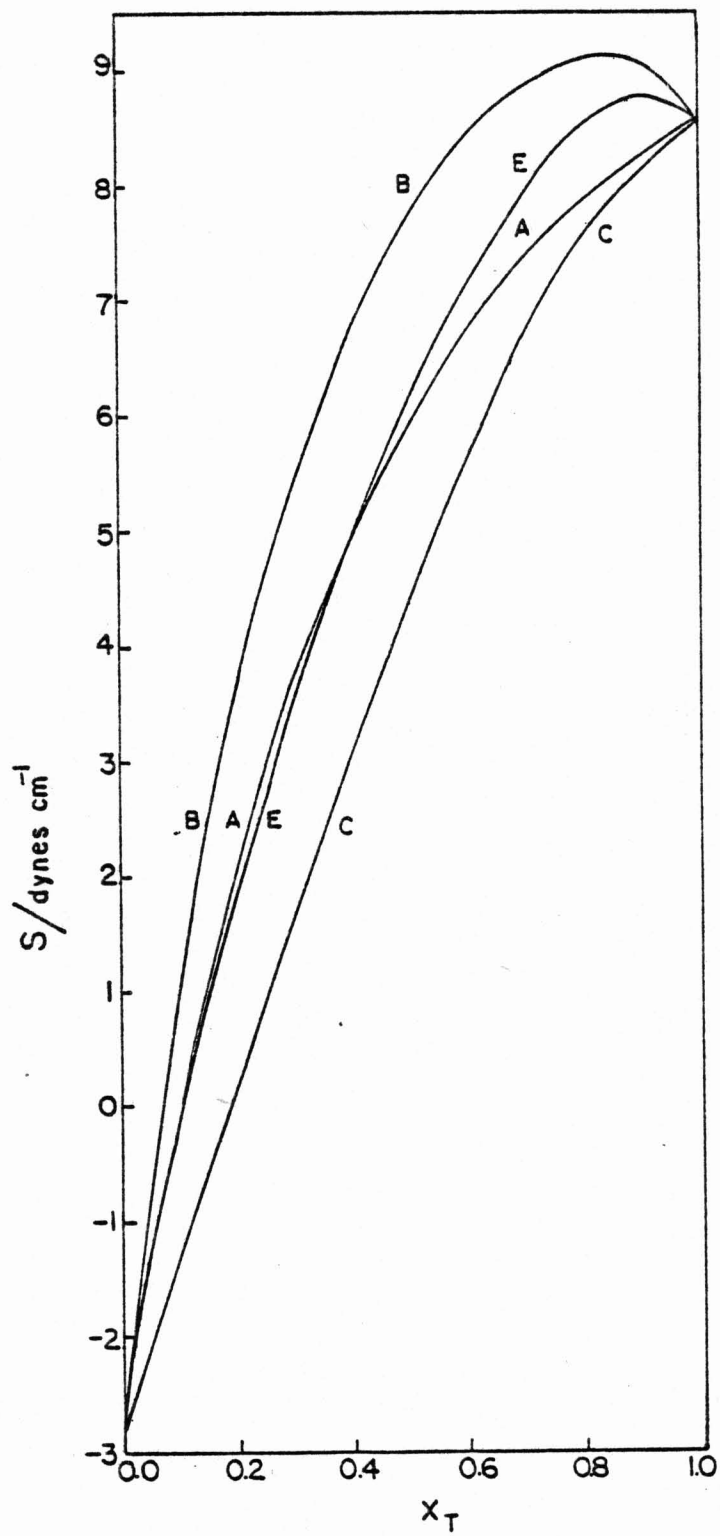
Figure 14. Initial spreading coefficients,  $S$ , of toluene-decane mixtures on water at 25°C plotted as a function of the mole fraction of toluene in the organic mixture.

E - experimental

A - calculated from equation 7

B - calculated from equation 9

C - calculated from equation 17



appears in the experimental curve. The Prigogine-Marechal equation, which takes size differences into account, predicts a much lower value of  $S$  than was found experimentally. When the activity coefficient is introduced (equation (9)) a maximum appears, although the experimental  $S$  data are not reproduced. Spreading on water of dilute solutions of decane in benzene is thermodynamically more favorable than either the spreading of pure benzene on water or the spreading of concentrated decane solutions in benzene on water. Non-idealities occurring in the bulk may qualitatively account for this effect. The lowering of the maximum with lengthening of the alkyl side chain is consistent with the decrease in activity coefficients<sup>59</sup>, the more similar size of the two components, and the decreased tendency to adsorb to the oil-water interface.

### C. Excess Volumes of Mixing

The drop-volume technique for measuring surface tension required the measurement of solution densities for the decane-aromatic mixtures. These data permit a limited evaluation of non-ideality effects on the volume of mixing. The excess molar volumes ( $V^E$ ), which are measures of the non-ideality of mixing, were calculated using equation (19).<sup>64</sup>

$$V^E = \frac{M_1 x_1 + M_2 x_2}{\rho} - \frac{M_1 x_1}{\rho_1} - \frac{M_2 x_2}{\rho_2} \quad (19)$$

where,  $M_i$  is the molecular weight of component  $i$ ,  
 $x_i$  is the mole fraction of component  $i$ , and  
 $\rho$  is the density.

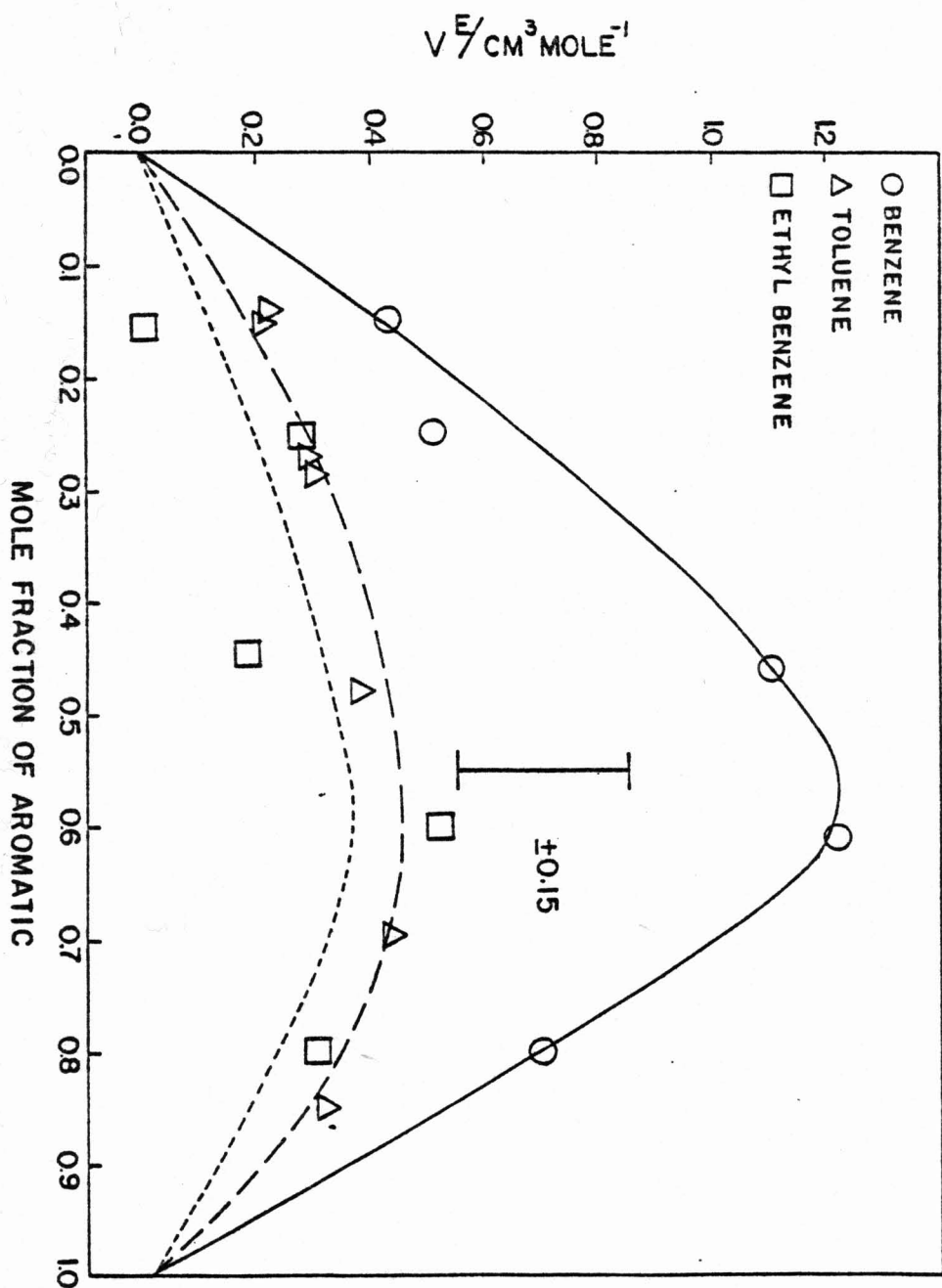
Figure 15 shows that a non-ideality of mixing exists since  $V^E$  is significant, especially in the case of benzene. However the effect observed corresponds to a maximum of 1% in density. The assumption of zero volume change on mixing, then, is reasonable. The excess volume decreases significantly between benzene and toluene. The ethylbenzene data showed the largest scatter through the mean deviation around a smooth curve. As noted in the results section the error is no greater than 0.2% in density, however. The excess volume data for ethylbenzene are consistent with the trend established by benzene and toluene. Jain and co-workers<sup>64</sup> noted similar volume changes on mixing for benzene-n-alkane systems. They found that the excess volume decreased as the alkyl chain length was decreased.

#### D. Interfacial Excess Quantities and Application to Micellar Solubilization

For surface tension data model D fits the data well enough for surface excess quantities to be calculated from model parameters, if needed. No model was found to be

Figure 15. Excess molar volumes of benzene-decane, toluene-decane, and ethylbenzene-decane mixtures at 25°C plotted as a function of the mole fraction of the aromatic component.

The error bar indicates the expected average error in molar volume based upon a 0.1% error in density. This was shown to be in close agreement with the average value of the 95% confidence limits around each point.



adequate for the interfacial tension data, however, and the experimental data had to be used. In this section results of direct determination of surface excess quantities from interfacial tension data are reported. These excess quantities are also of interest for comparing the relative adsorption of the aromatic species to bulk interfaces, and in using such data for the application of the two-state model for lipid assemblies.

Gibbs's approach<sup>65,66</sup> to surface properties uses excess quantities relative to the bulk. He showed that at constant temperature for a binary mixture

$$d\gamma = -\Gamma_1^\sigma d\mu_1 - \Gamma_2^\sigma d\mu_2 = -\frac{n_1^\sigma}{A} d\mu_1 - \frac{n_2^\sigma}{A} d\mu_2 \quad (20)$$

where  $n_i^\sigma$  is the number of moles of component  $i$  at the surface in excess of what would have been there had the dividing surface between the phases been located in the bulk,

$A$  is the surface area, and

$\Gamma_i^\sigma (= n_i^\sigma/A)$  is the surface excess of component  $i$ .

At constant temperature and pressure the Gibbs-Duhem equation for a binary mixture is

$$N_1 d\mu_1 = -N_2 d\mu_2 \quad (21)$$

where  $N_i$  is the number of moles of component  $i$ .

Substituting equation (21) into equation (20) gives

$$-\frac{d\gamma}{d\mu_2} = [\Gamma_2^\sigma - \left(\frac{N_2}{N_1}\right)\Gamma_1^\sigma] \quad (22)$$

The quantities  $\Gamma_1^\sigma$  and  $\Gamma_2^\sigma$  cannot be determined independently without an additional assumption or convention about the Gibbs dividing surface. If this surface is chosen such that  $\Gamma_1^\sigma$  is zero, then

$$-\frac{d\gamma}{d\mu_2} = -\frac{d\gamma}{RT d \ln a_2} = \Gamma_2^1. \quad (23)$$

$\Gamma_2^1$  is the number of moles of component 2 per unit area of the surface region in excess of the number of moles of component 2 in a region of the bulk which contains the same number of moles of component one. The size of the bulk region to which the surface is compared is determined by the number of moles of component one. Surface and bulk regions containing the same numbers of moles of component one are compared. The difference in the number of moles of component two is the algebraic surface excess.

Although  $\Gamma_2^1$  is perhaps the most frequently used quantity in describing adsorption of surfactants and other highly surface active second components, for mixtures of liquids such as the ones being discussed here, a number of other conventions have been useful. For application to the thermodynamic descriptions of small lipid assemblies

containing surface active solutes, some of the other conventions may actually be of greater interest. For example, bulk and surface regions containing the same number of total moles may also be compared. In this case  $\sum_i \Gamma_i^N = 0$ , where N refers to this convention of choosing the surface, namely the N convention. The required condition can be expressed in terms of  $\Gamma^1$  since  $\sum_i x_i \Gamma_i^1 = 0$  so that  $\Gamma_2^N = x_1 \Gamma_2^1$  (24). Also bulk and surface regions containing exactly the same volume may be compared. In this case  $\sum_i V_i \Gamma_i^V = 0$ , where  $V_i$  is the partial molar volume of component i. The sum of the volumes of each component going to the surface is zero. It can be shown that  $\Gamma_2^V = (V_1 \Gamma_2^N) / (x_1 V_1 + x_2 V_2)$  (25) for a binary mixture. Guggenheim and Adam<sup>65</sup> have suggested that this convention is the only one for which the geometrical surface coincides exactly with the physical boundary of the liquid.

The experimental estimates of  $\Gamma^D$ ,  $\Gamma^N$ , and  $\Gamma^V$  are shown in Figures 16, 17, and 18. (Subscripts B, T, and E are used to indicate benzene, toluene, and ethylbenzene; and superscript D is used to indicate the  $\Gamma_2^1$  convention with decane as component one.) These values were determined by graphical differentiation of the  $\gamma$  vs. x data and use of the activity coefficient from solubility parameter theory. For the differentiation of  $\gamma$  vs. x data, when contiguous points were too close for  $\Delta\gamma/\Delta x$  values to be determined to any reasonable degree of precision, data points one or two

Figure 16. Interfacial excess quantities of benzene at the benzene-decane mixture-water interface plotted as a function of the mole fraction of benzene in the organic phase at 25°C.

$\Gamma_B^D$  - calculated from equation 23

$\Gamma_B^N$  - calculated from equation 24

$\Gamma_B^V$  - calculated from equation 25

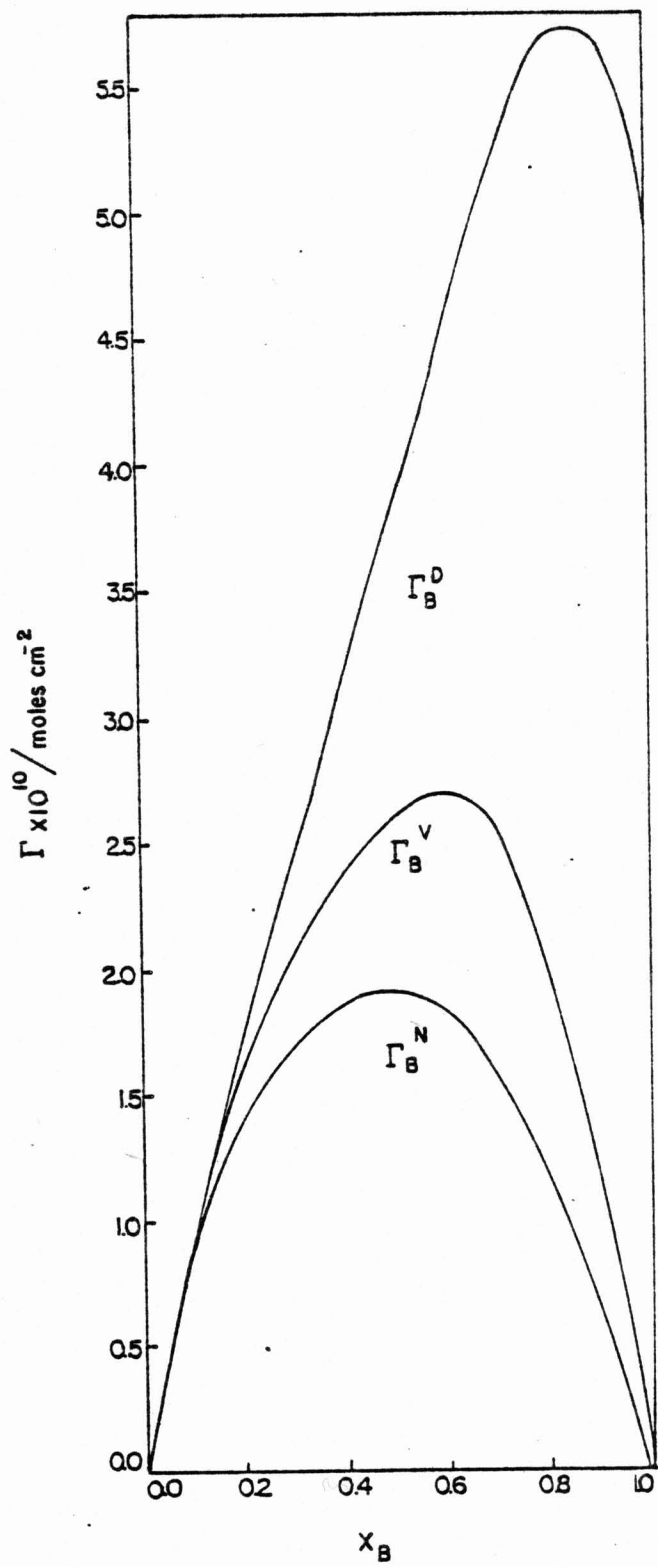


Figure 17. Interfacial excess quantities of toluene at the toluene-decane mixture-water interface plotted as a function of the mole fraction of toluene in the organic phase at 25°C.

$\Gamma_T^D$  - calculated from equation 23

$\Gamma_T^N$  - calculated from equation 24

$\Gamma_T^V$  - calculated from equation 25

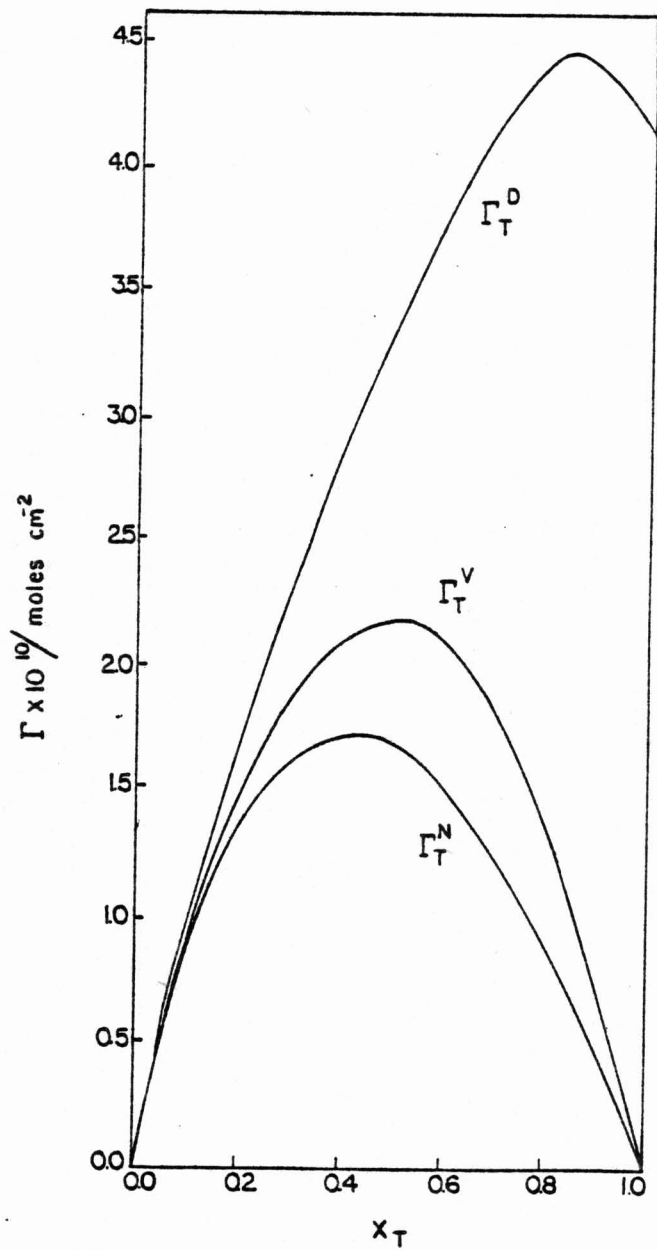
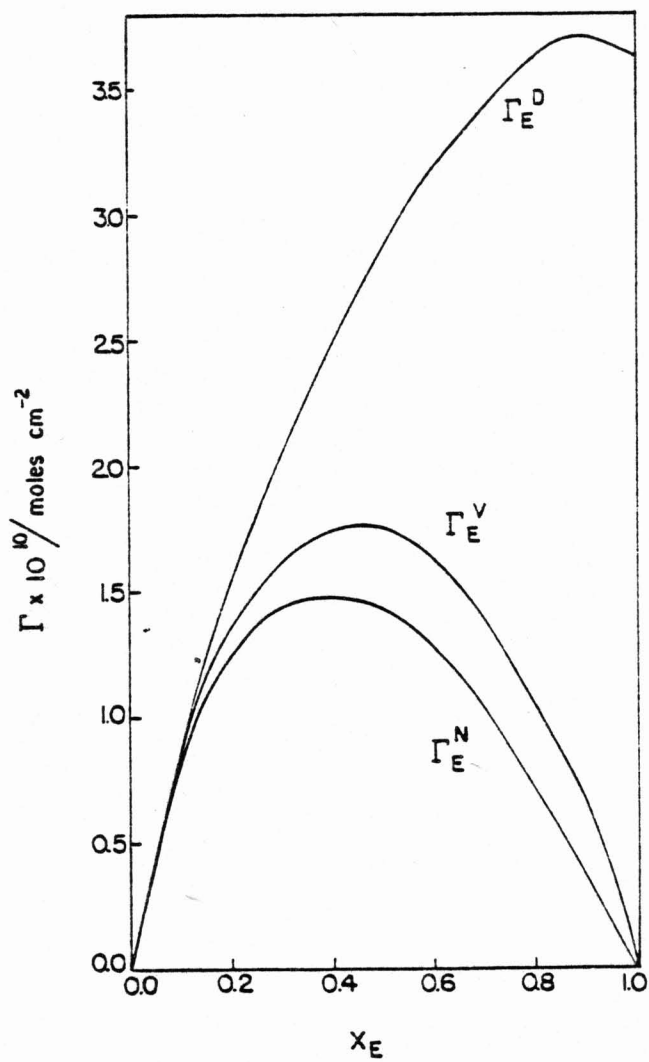


Figure 18. Interfacial excess quantities of ethylbenzene at the ethylbenzene-decane mixture-water interface plotted as a function of the mole fraction of ethylbenzene in the organic phase at 25°C.

$\Gamma_E^D$  - calculated from equation 23

$\Gamma_E^N$  - calculated from equation 24

$\Gamma_E^V$  - calculated from equation 25



measurements away from the original were used to give more reliable estimates of  $\Delta\gamma/\Delta x$ . A large number of such values were then used to define a mean curve. A check on this curve was obtained by graphical integration<sup>67,68</sup> of the final smooth differential curve over the whole composition range. Because the differential curve was already smoothed out, this integration was relatively precise. The integrated curves have been plotted in Figures 4, 5, and 6, where the  $\gamma$  vs.  $x$  data are displayed. The integrated curves describe the experimental data within experimental error in general. This procedure was laborious but was preferred to the procedure often employed, namely fitting  $\gamma$  vs.  $x$  curves to arbitrary algebraic forms, and, then, differentiating the resultant relations. Non-uniform random and systematic errors are involved in the experimental  $\gamma$  vs.  $x$  curves. Fitted equations can magnify errors in slopes at the extreme of concentration although the overall fit may be good.

$\Gamma^D$  curves in Figures 16-18 show slight maxima. In dilute solutions the differences between  $\Gamma^D$ ,  $\Gamma^N$ , and  $\Gamma^V$  are small, as expected. At high concentrations major absolute and relative differences appear because  $\Gamma^V$  and  $\Gamma^N$  must go to zero when  $x$  goes to unity. The surface activity of these aromatic compounds is indeed mild when compared to typical surfactants. At low mole fraction the surface excess shows a linear relationship with mole fraction. At

$x = 0.01$ , for example, the surface excess is about  $1.7 \times 10^{-11}$  moles  $\text{cm}^{-2}$  or about  $980 \text{ \AA}^2 \text{ molecule}^{-1}$  for benzene. Typical surfactants occupy about  $50-100 \text{ \AA}^2 \text{ molecule}^{-1}$  at concentrations far below a mole fraction of  $0.01$ .<sup>21</sup>

Comparison of the graphs for the different compounds indicates that the increase of alkyl chain length leads to decreased relative adsorption to the organic liquid-water interface. The Prigogine-Marechal<sup>37</sup> parallel layer model could predict this behavior from the values of  $\phi_1^S$  and  $\phi_1$  at any composition. Since a one parameter approach to the Prigogine model could not predict the value of the interfacial tension at every composition, the calculated values of  $\phi_1^S$  based on that model are not considered here. Further investigation of the usefulness of the parallel layer model for estimating adsorption will be necessary.

Each convention gives a value of the excess at an arbitrarily chosen dividing surface. As can be seen from Figures 16, 17, and 18, in dilute solutions of the aromatic compounds, all of the conventions predict the same value for the surface excess. At higher values of  $x$  the  $\Gamma$  plots clearly indicate that there are differences in the dividing surfaces chosen by the different conventions. An examination and comparison of the three conventions mentioned should provide a qualitative indication of the change in surface excess with concentration.

As pointed out in the introduction, one of the major

purposes of this work was the estimation of interfacial excess quantities to be used for determination of the distribution of solubilizates between a decane-like micellar core and the micelle-water interface. As a model a mole of SDS micelles is considered. Huisman<sup>69</sup> has determined the aggregation number of SDS micelles in aqueous solution to be 57.3. Assuming, on the basis of density measurements<sup>61</sup>, that the dodecyl group of SDS has an approximate molar volume of  $218 \text{ ml mole}^{-1}$ , the radius of the hydrocarbon core of a spherical SDS micelle is calculated to be  $17.04 \text{ \AA}^2$ . If the excess molar volume of mixing is assumed to be negligible and assuming the aggregation number does not change upon solubilization, the change in the core volume can be calculated using the bulk values for the molar volume of the aromatic component. From a knowledge of the core volume, the surface area of the core of a mole of spherical micelles can be determined, and multiplied by the surface excess to yield the total number of moles of solubilizate at the surface of a mole of micelles. Table XI displays the results of these calculations in terms of the fraction,  $f$ , adsorbed and the ratio,  $R$ , of the amount at the surface to the amount in the core for each of the three compounds studied and for each of the conventions examined at selected values of the mole fraction of solubilizate in the core.

A number of points regarding the results in Table XI

Table XI. Distribution of Solubilizate between Adsorbed and Dissolved States of an SDS Micelle on the Basis of the Model for Micellar Solubilization Described in the Text (p. 91).

<u>Solubilizate</u>	<u>Mole Fraction</u>		<u>Fraction Adsorbed, f</u>			<u>Adsorbed to Dissolved Ratio, R</u>		
	<u>Core</u>	<u>Total<sup>a</sup></u>	<u><math>\Gamma^D</math></u>	<u><math>\Gamma^N</math></u>	<u><math>\Gamma^V</math></u>	<u><math>\Gamma^D</math></u>	<u><math>\Gamma^N</math></u>	<u><math>\Gamma^V</math></u>
Benzene	0.001	0.0061	0.84	0.84	0.84	5.2	5.2	5.2
	0.04	0.18	0.81	0.81	0.81	4.3	4.2	4.2
	0.10	0.33	0.78	0.76	0.77	3.5	3.2	3.4
	0.20	0.48	0.74	0.70	0.72	2.9	2.3	2.6
	0.40	0.64	0.68	0.56	0.62	2.1	1.2	1.6
Toluene	0.001	0.0056	0.82	0.82	0.82	4.6	4.6	4.6
	0.04	0.17	0.80	0.80	0.80	4.1	3.9	4.0
	0.10	0.32	0.78	0.76	0.76	3.4	3.1	3.2
	0.30	0.55	0.70	0.62	0.66	2.4	1.6	1.9
	0.40	0.62	0.66	0.54	0.59	2.0	1.2	1.4
Ethylbenzene	0.001	0.0054	0.82	0.82	0.82	4.4	4.4	4.4
	0.04	0.16	0.80	0.80	0.80	3.8	3.7	3.8
	0.10	0.31	0.77	0.75	0.75	3.3	3.0	3.0
	0.40	0.60	0.64	0.51	0.55	1.8	1.0	1.2

<sup>a</sup>Calculated on the basis of  $\Gamma^V$ .

should be emphasized. A significant amount of the solubilize is in the adsorbed state at the micelle-water interface. This amount decreases with increasing core concentration according to each convention. The values of the total mole fraction of solubilize indicate that the range examined encompasses the full extent of solubilization expected for micellar systems (0.47 in SDS and 0.7 in CTAB, for example). The relative adsorption decreases with increasing alkyl substitution.

It should be mentioned that another surface excess<sup>65</sup> convention was also examined. This convention assumes that the interface is a monolayer and introduces the restriction that  $A_1 \Gamma_1^u + A_2 \Gamma_2^u = 1$  for a binary mixture, where  $A_i$  is the molar area of component  $i$ , and  $\Gamma_i^u$  is the surface excess of component  $i$ .

It can be shown that  $\Gamma_1^u = (A_2 \Gamma_1^N + N_1) / (N_1 A_1 + N_2 A_2)$ . The values of  $\Gamma^u$  for the composition regions applicable to micelles were found to be bracketed by the  $\Gamma^N$  and  $\Gamma^V$  values if the same  $A_i$  values used in assessing the Prigogine-Marechal model were employed.

Two types of data on micellar systems mentioned in the introduction can be compared with the results obtained in Table XI. First, the spectroscopic data of Mukerjee and Cardinal<sup>20,21</sup>, and Rehfeld<sup>11,12</sup> can be examined. In attempting to interpret their data, Mukerjee and Cardinal<sup>20,21</sup> developed a parameter  $H_{eff}$  defined as the

ratio of the molar volume of dipoles in a solvent to that of water (55.4 moles/L). Thus water has an  $H_{eff}$  of one and decane's  $H_{eff}$  is zero. This parameter was found to vary monotonically with the dielectric constant of the solvent and with the spectral parameters chosen to study the average microenvironment of the solubilized species.  $H_{eff}$  provides a measure of the hydrophilicity of the medium. Molecules at the micelle-water interface should be experiencing a predominantly aqueous environment especially if hydrogen bonding is occurring. Those molecules in the core would have an  $H_{eff}$  of zero due to the decane-like environment. Therefore, the space-averaged  $H_{eff}$  given by spectroscopic parameters should be closely related to the fraction adsorbed at the micelle-water interface. The values of  $f$ , the fraction adsorbed at the micelle-water interface, given in Table XI indicate that at low concentrations of benzene in SDS micelles behaving according to the model presented here 83.8% of the benzene is at the interface. A dilute solution of benzene in SDS micelles was found by Mukerjee and Cardinal<sup>21</sup> to have an  $H_{eff}$  value, determined spectrophotometrically, of 0.65. Rehfeld<sup>11</sup> had studied saturated solutions of benzene in a similar manner. From his results an  $H_{eff}$  value of  $0.3 \pm 0.1$  could be determined for benzene in SDS micelles. In the region of saturation (0.47 mole fraction), the fraction of benzene at the interface is about 0.7 according to the present model

depending upon the convention employed.

Table XII accounts for the fraction of the micelle surface which is occupied by sulfate head groups and therefore should be unavailable for benzene or alkylbenzene adsorption. The radius of the head group was taken to be approximately  $3 \text{ \AA}$  based on the S-O bond distance of  $\text{SO}_4^{=}$ ,  $1.5 \text{ \AA}$ , and the van der Waals radius of oxygen,  $\sim 1.4 \text{ \AA}$ .<sup>70</sup> The values of  $f$  for benzene at low concentration in micellar solutions, 0.741, and near saturation, 0.505 ( $r^N$ ), tend in the direction of closer quantitative agreement with the  $H_{\text{eff}}$  parameters determined from the data of Mukerjee and Cardinal<sup>20,21</sup>, and Rehfeld<sup>11</sup>.

Ethylbenzene at low concentration in SDS micelles was also examined by Mukerjee and Cardinal.<sup>21</sup> The value of  $H_{\text{eff}}$  was determined to be 0.55. The values of  $f$  from Tables XI and XII, 0.815 and 0.711, respectively, also fall short of quantitative agreement. Compared with the  $f$  value for benzene, 0.838, the fraction of ethylbenzene at the surface tends in the direction of decreasing  $H_{\text{eff}}$  with increasing alkyl chain length of the solubilizate.

By their very nature the viscosity data of Eriksson and Gillberg<sup>16</sup>, Smith and Alexander<sup>25</sup>, and Mukerjee and Manabe<sup>26</sup> could not be expected to be simply interpreted by the above model. Viscosity changes are considered to be due to sphere-to-rod transition<sup>16,25,28</sup> which the present model neglects. The instability of rod-shaped micelles

Table XII. Distribution of Solubilizate between Adsorbed and Dissolved States of an SDS Micelle on the Basis of the Model for Micellar Solubilization Described in the Text (p. 91) and Assuming that a Fraction of the Hydrocarbon Core Surface is Unavailable for Adsorption due to the Area Occupied by the Sulfate Head Groups.

Solubilizate	Mole Fraction		Fraction of Surface Available	Fraction Adsorbed, f		Adsorbed to Dissolved Ratio, R	
	Core	Total <sup>a</sup>		$\Gamma^N$	$\Gamma^V$	$\Gamma^N$	$\Gamma^V$
Benzene	0.001	0.0039	0.56	0.74	0.74	2.9	2.9
	0.1	0.24	0.57	0.64	0.66	1.8	1.9
	0.3	0.49	0.60	0.60	0.55	1.0	1.2
Toluene	0.001	0.0036	0.56	0.72	0.72	2.6	2.6
	0.1	0.24	0.57	0.64	0.65	1.8	1.8
	0.4	0.56	0.63	0.43	0.48	0.75	0.9
Ethylbenzene	0.001	0.0034	0.56	0.71	0.71	2.5	2.5
	0.1	0.23	0.57	0.63	0.64	1.7	1.8
	0.25	0.42	0.60	0.52	0.54	1.1	1.2

<sup>a</sup>Calculated on the basis of  $\Gamma^V$ .

with respect to spheres has been explained to be due primarily to the high charge density in the head group region of ionic micelles.<sup>27</sup> The presence of solubilize at the micellar surface can, therefore, stabilize the rod-shaped micelle by decreasing head group interactions.<sup>27</sup> As pointed out by Mukerjee<sup>7</sup> on the basis of interfacial activity effects, at high solubilize concentrations the ratio of surface to core solubilize is likely to be lower than in dilute micellar solutions. This is consistent with the decreasing R values calculated by the present model in Tables XI and XII. Mukerjee<sup>7</sup> reasoned that the micelle could become a swollen sphere as core solubilization became more favored compared to the interface ( $R < 1$ ). If the solubilize is predominantly at the surface of the micelle, thereby stabilizing the rod-shaped micelle, the micellar radius may not change and the micelle may even become thinner.<sup>25</sup> However, when a large fraction of solubilize is in the core, the micelle can swell spherically.<sup>7</sup> Swollen spherical micelles would not be expected to exhibit the high viscosity of rods. The maximum in viscosity would then correspond to a rod-to-sphere transition effected by the change in surface to core ratio.<sup>7</sup>

Although the present model cannot deal quantitatively with the data generated in CPC micelles, the marked decrease in R with increasing solubilize concentration shown in Tables XI and XII is consistent with a shift to a

predominantly core location of the solubilizate at high concentrations of solubilizate. For example, by coincidence the R values for toluene presented in Table XII are found to fall below one at a total mole fraction just beyond the maximum point found by Mukerjee and Manabe for CPC micelles in 0.5M NaCl solution. However, an order of magnitude difference in the specific viscosity maximum between toluene and ethylbenzene was also noted. The maximum for ethylbenzene occurred at a lower total mole fraction of the solubilizate. The R values calculated on the basis of the present model alone are unable to account for this difference.

Indeed the sphere-to-rod transition process can be markedly influenced by seemingly minor effects. Mukerjee<sup>27</sup> has shown on the basis of the multiple equilibrium model for micelle formation that changing the region of anti-cooperativity of self-association by one monomer unit markedly influenced the size distribution of micelles. Anti-cooperative regions for ionic micelles are due primarily to interactions of charged head groups. In the anti-cooperative region further addition of monomers to micelles becomes progressively more unfavorable with each monomer added. The ability of a solubilizate at the micelle-water interface to change the anti-cooperative region by even a small amount could stabilize the formation of large rod-shaped micelles. Therefore, in addition to

the obvious shortcomings of the present model for analyzing sphere-to-rod transitions, analysis of viscosity data for micellar systems will require consideration of the subtleties associated with this change in micelle size and geometry.

The zeroth order model presented here can be amended in a number of general ways so as to bear closer resemblance to real micellar systems. The effect of curvature on the interfacial tension of the micelle and the resultant effects on adsorption should be considered.<sup>28</sup> The Laplace pressure which influences the distribution of molecules between the continuous phase and the micelle is a result of the micelle's curvature. A Laplace pressure of 296 atm was found by Mukerjee<sup>7</sup> to reproduce within  $\pm 5\%$  the differences in  $\Delta G$  of transfer for hydrocarbon gases from water to bulk hydrocarbon liquids and from water to SDS micelles. The Laplace pressure then accounted for much of the difference between solubilization of these solutes in micelles and in bulk liquids. This value for the Laplace pressure,  $P$  ( $= 2\gamma r^{-1}$ ), suggested an interfacial tension of 31.5 dynes  $\text{cm}^{-1}$  for the SDS micelle in 0.1M NaCl.

The activity coefficients used in this study were determined from solubility parameter theory.<sup>59</sup> Based on the values determined<sup>58</sup> for other alkane-benzene systems, the actual activity coefficients are likely to be higher than solubility parameter theory would predict. Activity

coefficients for benzene solubilized by micelles have been determined.<sup>71</sup> These values will prove useful for modelling micellar solubilization and for assessing the usefulness of bulk liquids for describing intramicellar interactions.

The micellar solubilization model presented here considers only SDS at a fixed aggregation number. Upon solubilization of alkane and aromatic solutes the aggregation numbers of micelles have been shown to increase. Almgren and Swarup<sup>72</sup> have recently reported an increase in aggregation number of SDS micelles at 22°C from 69.6 with no solubilizate to 89.0 in the presence of toluene at 0.31 mole fraction in the micelle.

Although, as with most working models, refinements can be made, the implications of the results remain significant. In any lipid assembly having a high surface-to-volume ratio, the surface activity of a solubilizate will influence the distribution of the solubilizate between the lipid assembly and the aqueous medium. As a result, the transport of small slightly polar molecules through lipid bilayers will be affected. The composition dependence of the fractional amount at the surface can influence the capacity of the lipid assembly to solubilize a compound. The stability of solubilized compounds whose reactivity is dependent upon exposure to hydrophilic species (e.g.,  $H^+$ ) will also be affected.

## V. CONCLUSIONS

1. Surface tension vs. composition curves for decane-benzene, decane-toluene, and decane-ethylbenzene mixtures are described by the Prigogine-Marechal parallel layer model, which allows for size differences and interactions between the components of the mixture, using an interaction parameter,  $\beta$ , which is lower than that predicted from regular solution theory.

2. Interfacial tensions of these systems are not described by the Prigogine-Marechal theory using a single adjustable parameter over the whole composition range. At low concentrations of aromatic component in decane a higher  $\beta$  value is found than at high concentrations. In all cases the parameters for interfacial tensions are higher than those determined from surface tensions. Hydrogen bonding between the aromatics and water may account for this effect.

3. Excess mixing volumes for these systems decrease with alkyl substitution on the aromatic ring.

4. The relative adsorption of the aromatics to the decane-water interface is mild yet significant. The adsorption decreases with increasing chain length of the

alkyl substituent.

5. Using the bulk liquid values, the fractional amounts of aromatic solubilizate which would be adsorbed to the surface of a modelled SDS micelle have been shown to decrease, according to each convention examined for choosing the dividing surface, as more solubilizate is added to the micellar core.

6. The values determined for the adsorption to the micelle-water interface of the aromatic compounds studied are in qualitative agreement with the results of spectroscopic and viscometric studies and the trends expected from the two-state model for micellar solubilization.

## VI. REFERENCES

1. Fendler, J. H., "Membrane Mimetic Chemistry," Wiley, New York (1982).
2. a. Mukerjee, P., *Adv. Coll. Interf. Sci.*, 1, 241 (1967).  
b. Tanford, C., "The Hydrophobic Effect: Formation of Micelles and Biological Membranes," Wiley, New York (1973).
3. Hoffmann, A. F., *Biochem. J.*, 89, 57 (1963).
4. Knight, C. G., ed., "Liposomes: From Physical Structure to Therapeutic Applications," Elsevier/North-Holland, New York (1981).
5. Florence, A. T., in "Techniques of Solubilization of Drugs," S. Yalkowsky, ed., Dekker, New York (1981).
6. Fendler, J. H. and Fendler, E., "Catalysis in Micellar and Macromolecular Systems," Academic Press, New York (1975).
7. Mukerjee, P., in "Solution Chemistry of Surfactants," K. L. Mittal, ed., 1, Plenum, New York (1979).
8. McBain, M. E. L. and Hutchinson, E., "Solubilization and Related Phenomena," Academic Press, New York (1955).
9. Elworthy, P. H., Florence, A. T. and MacFarlane, C. B., "Solubilization by Surface Active Agents," Chapman and Hall, London (1968).

10. Klevens, H. B., Chem. Rev., 47, 1 (1950).
11. Rehfeld, S., J. Phys. Chem., 74, 117 (1970).
12. Rehfeld, S., J. Phys. Chem., 75, 3905 (1970).
13. Mukerjee, P., J. Phys. Chem., 74, 3824 (1970).
14. Rowlinson, J. S., "Liquids and Liquid Mixtures," Butterworth, London (1969).
15. Riegelman, S., Allawalla, N. A., Hrenoff, M. K. and Strait, L. A., J. Coll. Sci., 13, 208 (1958).
16. Eriksson, J. C. and Gillberg, G., Acta Chem. Scand., 20, 2019 (1966).
17. Fendler, J. H. and Patterson, L. K., J. Phys. Chem., 74, 4608 (1970).
18. Fendler, E. J., Day, C. L., and Fendler, J. H., J. Phys. Chem., 76, 1460 (1972).
19. Fox, K. K., Robb, I. D. and Smith, R., Faraday Trans. I, 68, 445 (1972).
20. Cardinal, J. R. and Mukerjee, P., J. Phys. Chem., 82, 1614 (1978).
21. Mukerjee, P. and Cardinal, J. R., J. Phys. Chem., 82, 1620 (1978).
22. Simon, S. A., McDaniel, R. V. and McIntosh, T. J., J. Phys. Chem., 86, 1449 (1982).
23. Jobe, D. V., Reinsborough, V. C. and White, P. J., Can. J. Chem., 60, 279 (1982).
24. Rehfeld, S. J., J. Phys. Chem., 71, 738 (1967).

25. Smith, M. B. and Alexander, A. E., in "Proc. 2nd Int. Cong. Surface Activity," Vol. 1, p. 311, Butterworth, London (1957).
26. Mukerjee, P. and Manabe, M., unpublished work.
27. Mukerjee, P., in "Micellization, Solubilization and Microemulsions," 1, p. 171, K. L. Mittal, ed., Plenum, New York (1977).
- 28. Mukerjee, P., Pure and Applied Chem., 52, 1317(1980).
29. Eberhart, J. G., J. Phys. Chem., 70, 1183 (1966).
30. Meissner, H. P. and Michaels, A. S., Ind. Eng. Chem., 41, 2782 (1949).
31. Butler, J. A. V., Proc. Roy. Soc. A, 135, 348 (1932).
32. Croxton, C., "Statistical Mechanics of the Liquid Surface," Wiley, New York (1980).
33. Belton, J. W. and Evans, M. G., Trans. Faraday Soc., 41, 1 (1945).
34. Guggenheim, E. A., Trans. Faraday Soc., 41, 150 (1945).
35. Hoar, T. P. and Melford, D. A., Trans. Faraday Soc., 53, 315 (1957).
36. Hildebrand, J. H. and Scott, R. L., "The Solubility of Nonelectrolytes," Reinhold, New York (1950).
37. Prigogine, I. and Marechal, J., J. Coll. Sci., 7, 122 (1952).
38. Defay, R., Prigogine, I., Bellemans, A. and Everett, D. H., "Surface Tension and Adsorption," Wiley, New York (1966).

39. Sprow, F. B. and Prausnitz, J. M., *Trans. Faraday Soc.*, 55, 2013 (1959).
40. Eckert, C. A. and Prausnitz, I., *A. I. Chem. E. J.*, 10, 677 (1964).
41. Gaines, G. L., Jr., *J. Phys. Chem.*, 73, 3143 (1979).
42. Schmidt, R. L., Randall, J. C. and Clever, H. L., *J. Phys. Chem.*, 70, 3912 (1966).
43. Gaines, G. L., Jr., *Trans. Faraday Soc.*, 65, 2370 (1969).
44. Aveyard, R., *Trans. Faraday Soc.*, 63, 2778 (1967).
45. Aveyard, R. and Haydon, D. A., "An Introduction to the Principles of Surface Chemistry," Cambridge University Press, New York (1973).
46. Handa, T. and Mukerjee, P., *J. Phys. Chem.*, 85, 3916 (1981).
47. Edmonds, B. and McLure, I. A., *J. Chem. Soc. Faraday Trans.*, 1., 78, 3319 (1982).
48. Kaelble, D. H., "Physical Chemistry of Adhesion," Wiley, New York (1971).
49. Halper, L. P., Timmons, C. O. and Zisman, W., *J. Coll. Interf. Sci.*, 38, 511 (1972).
50. Jasper, J. J., *J. Phys. Chem. Ref. Data*, 1, 841 (1972).
51. Rossini, F. D., et al., "Selected Values of Physical and Thermodynamic Properties of Hydrocarbons and Related Compounds," *Am. Pet. Inst., Res. Proj.* 44 (1953).

52. Aveyard, R. and Haydon, D. A., *Trans. Faraday Soc.*, 61, 2255 (1965).
53. Harkins, W. D. and Brown, F. E., *J. Am. Chem. Soc.*, 41, 499 (1919).
54. Ruysen, R., *Rec. Trav. Chim.*, 65, 580 (1946).
55. Bauer, N. and Levin, S. Z., in "Technique in Organic Chemistry," Vol. I, p. 157, Interscience, New York (1959).
56. Gillap, W. R., Weiner, N. D. and Gibaldi, M., *J. Am. Oil Chem. Soc.*, 44, 71 (1967).
57. Shewmaker, J. E., Vogler, C. E. and Washburn, E. R., *J. Phys. Chem.*, 58, 945 (1954).
58. Jain, D. V. S., Lark, B. S., Chamak, S. S. and Chander, P., *Ind. J. Chem.*, 8, 66 (1976).
59. Hildebrand, J. E., Prausnitz, J. M. and Scott, R. L., "Regular and Related Solutions: The Solubility of Gases, Liquids, and Solids," Van Nostrand, Reinhold, Co., New York (1970).
60. Yoshida, Z. and Osawa, E., *J. Am. Chem. Soc.*, 88, 4019 (1966).
61. Mellan, I., "Compatibility and Solubility," Noves Development Corp., Park Ridge, N.J. (1968).
62. Pimental, G. C. and McClellan, A. L., "The Hydrogen Bond," W. H. Freeman, Co., San Francisco (1960).
63. Hiemenz, P. C., "Principles of Colloid and Surface Chemistry," Dekker, New York (1977).

64. Jain, D. V. S., Gupta, V. K. and Lark, B. S., J. Chem. Thermodyn., 5, 451 (1973).
65. Guggenheim, E. A. and Adam, N. K., Proc. Roy. Soc. A., 139, 218 (1933).
66. Adamson, A. W., "Physical Chemistry of Surfaces," 4th Ed., Wiley, New York (1982), pp. 73-78.
67. Klotz, I. M. and Rosenberg, R. M., "Introduction to Chemical Thermodynamics," Benjamin, Reading, Ma. (1976).
68. Gibaldi, M. and Perrier, D., "Pharmacokinetics," Dekker, New York (1975).
69. Huisman, H. F., Proc. K. Ned. Akad. Wet. Ser. B., 67, 388 (1964).
70. Mukerjee, P., J. Phys. Chem., 65, 740 (1961).
71. Tucker, E. E. and Christian, S. D., Faraday Symposia of the Chemical Society, No. 17, 1 (1982).
72. Almgren, M. and Swarup, S., J. Phys. Chem., 86, 4212 (1982).

SURFACE PROPERTIES OF BINARY MIXTURES OF BENZENE, TOLUENE,  
AND ETHYLBENZENE WITH DECANE AT THE AIR-LIQUID  
AND WATER-LIQUID INTERFACES

BY

MICHAEL J. GUMKOWSKI

A thesis submitted in partial fulfillment of  
the requirements for the degree of

MASTER OF SCIENCE  
(Pharmacy)

at the

UNIVERSITY OF WISCONSIN-MADISON

1983

APPROVED:

Paul L. Munkin

Kenneth A. Combs

George Zografis

DATE:

May 19 1983